ISSN 1063-7796, Physics of Particles and Nuclei, 2016, Vol. 47, No. 1, pp. 108–133. © Pleiades Publishing, Ltd., 2016.
Original Russian Text © B.Zh. Zalikhanov, 2016, published in Fizika Elementarnykh Chastits i Atomnogo Yadra, 2016, Vol. 47, No. 1.

From an Electron Avalanche to the Lightning Discharge

B. Zh. Zalikhanov

Joint Institute for Nuclear Research, Dubna, Moscow oblast, 141980 Russia
e-mail: zalikhanov@jinr.ru

Abstract—The goal of this work is to describe qualitatively the physics of processes which begin with an electron avalanche and finish in a lightning discharge. A streamer model is considered that is based on studies of the recently discovered processes occurring in the prestreamer region. The investigation and analysis of these processes enabled making the conclusion that they are, in essence, the attendant processes, which ensure the electron avalanche-to-streamer transition, and may be interpreted as a manifestation of properties of a double charge layer exposed to the external electric field. The pressing problems of physical processes which form a lightning discharge are considered from the standpoint of new ideas about the mechanism of the streamer formation and growth. Causes of the emergence of coherent super-high-frequency radiation of a leader and the neutron production in a lightning discharge are revealed that have not been explained so far in the theory of gas discharge. Based also on new ideas about the lightning discharge, a simple ball-lightning model, providing answers to almost allquestions formulated from numerous observations on the behavior of ball lightning, is offered, and the need of a new design of lightning protection instead of the traditional rod is discussed.

DOI: 10.1134/S1063779616010056

1. INTRODUCTION

For almost three hundred years, scientists have been seeking clues that could allow them to guess at the nature of lightning, but up to now, we had an incomplete understanding of this phenomenon. The observation and investigation of lightning discharges revealed numerous experimental facts which defy explanation from the viewpoint of state of the art of the gas discharge theory. In order to explain the causes of lightning, two theories are widely used.

The first one is based on the electrization of the ice or water particles rubbing against each other inside the thundercloud [1, 2]. While a thundery front forms, the falling pieces of ice encounter the warmer water drops gone upward by ascending flows. During their interaction, electrons break away from the drops and transfer to the ice pieces, due to which the water drops charge positively the upper region of the cloud, while the ice pieces charge its lower region negatively. The electric field strength of the thundercloud becomes of the order of 10^6 V/m.

Free electrons contained in the atmosphere receive in this field enough energy for ionizing the atmosphere's atoms and molecules. As a result, the electron avalanches arise, from which the glowing filamentary streamers grow with a length of a few tens of meters. Then the streamers merge and form a conductive channel called a lightning leader. A movement of the leader toward the ground occurs in separate steps, due to which it is called a stepped leader. A mean length of the step is ≈50 m. After formation of each step, a leader stops for the time of $\approx 5 \times 10^{-5}$ s, then again advances a few tens of meters. A bright glow covers the leader step which has formed; next, after a stop, it weakens in order to flare up again, but already together with the preceding steps. As observations show, a stepped leader passes a distance from the cloud to the ground (≈3–3.5 km) for $3 \times (10^{-2}–10^{-3})$ s, which corresponds to a speed of $10^7–10^8$ cm/s.

At the contact of the stepped leader with the ground, along the channel ionized by the leader, the return (bottom-up), or main, discharge of lightning, characterized by currents from tens to hundreds of thousands of amperes, follows, which exceeds noticeably the leader luminosity and has a high speed of propagation reaching $(0.3–0.5) \times 10^{10}$ cm/s. A channel temperature during the passage of main discharge may reach 20000–35000°C. The outer (visible) channel has a diameter of around a meter, while the inner (leader) channel, through which the current flows, is 1–6 cm in diameter. Each pulse duration is roughly 10^{-3} s, while pulse intervals are 10^{-2} s.

The second, more contemporary theory [3] is based on experiments conducted on aircraft and sounding balloons. From this theory it follows that lightning arises in the cloud at the electric field strength of no more than 3 kV/cm, though for the breakdown voltage of air at the heights of thundercloud formation, it is required that the electric field be of the order of magnitude higher: ≈20–30 kV/cm. The theory could not explain why this was happening. Another problem remaining unexplained in this theory was a sharp burst of gamma-radiation with the photon energy of up to 100 keV detected in a thundercloud in the late 1990s.

These problems are solved by A.V. Gurevich [4], who uses a new theory of electric breakdown that has become known as a breakdown caused by runaway electrons. In a thundercloud, an electrical discharge is caused by high-energy cosmic-ray particles, which create extensive air showers (EAS) in upper layers of the atmosphere. They consist of great number of charged and neutral high-energy particles which create the required fast electrons by ionizing the atmosphere's atoms and molecules. In the new theory, they are called the seed electrons. A peculiarity of interaction of a fast electron with slow electrons of the substance is that a deceleration force of the fast electron, determined by ionization losses, falls with a growth in its energy. Upon liberation from the forces that impede the motion, an electron begins to accelerate by the electric field. As soon as its energy reaches a value within the range 0.1–1 MeV, which is called the critical energy of runaway, the electron accelerates even faster [4].

Fast electrons traveling at a velocity close to the speed of light have a free path in air of an order of a few meters. Owing to the large free path, a fraction of these electrons may be accelerated by the electric field up to the energy that is much higher than the initial one. During a collision of these electrons with air molecules, some relativistic electrons will be liberated which will create an avalanche of "runaway" electrons. An aggregate of electron avalanches created thus along the path of runaway electrons will lead to an electrical breakdown of air at the atmospheric pressure. Moreover, this breakdown occurs at the electric field strength substantially smaller than the one required for a conventional air breakdown since the main ionization of atoms and molecules is carried out due to the energy loss of runaway electrons. So, at a pressure of 1 atm, the electric field threshold for a breakdown of 1 cm of air is on average 23 kV/cm, while for a runaway breakdown it is an order of magnitude less: 2.16 kV/cm. A breakdown itself is not yet lightning. A domain of breakdown presents the conducting plasma over many tens and hundreds of meters, which may become a germ of lightning. Experiments for verification of the theory of runaway breakdown have been conducted since 2002 at the Tien Shan Mountain Cosmic-Ray Station located at a height of 4000 m in mountains of Zailiiskii Alatau near Almaty. However, up to now, there has been no convincing experiment in support of this theory of discharge.

In this work, it will be shown that there is a mechanism of propagation of the ionization wave owing to the stored field energy between the double charge layers ("capacitors"), rather than due to an external electric field. This mechanism only depends on the power of supply source or thundercloud and is almost independent of the external field. A high electric field strength at heights of thundercloud formation, of the order of 10–30 kV/cm [5], is only required for development of the very first electron avalanches that give rise to a lightning discharge. Also without involving runaway electrons and special seed electrons produced by EAS particles, an explanation will be given to a majority of processes, occurring in a lightning discharge, with the use of simple mechanisms following from the structure of the ionized channel of lightning, which is offered by the author.

Observing and studying the lightning discharges have revealed many experimental facts that cannot be explained from the standpoint of the current state of the theory of gas discharge. First of all, it is caused by a lack of data on the inner structure of ionized channel.

A number of remarkable monographs and reviews are devoted to physics of the streamer and spark discharges [6–14]. As a result of generalization and analysis of experimental data, basic stages of development of the streamer and spark discharges are determined there, qualitative ideas about processes occurring in them are obtained, and areas of further research are outlined. However, we have not quite understood many problems so far and cannot give a clear answer to many questions. For example: how it is that a leader current at the contact with the ground grows instantly by two to three orders of magnitude, and what structure ensures the stability of a streamer and a leader, allowing them to form an ionized channel up to a few tens of kilometers in length?

The existing explanation of the indicated problems is based on the simplifying assumptions and actually allows only certain qualitative regularities to be revealed. As for the ionized channel structure, this issue almost is not discussed in literature. Moreover, a streamer is considered in [12] as the simplest structureless element of a spark discharge. Probably, the authors have assumed that the equality between the electric field, which arises inside the ionized channel, and the external field, in which a discharge is developing, is the sufficient condition providing the plasma channel stability.

The state of research concerning a spark breakdown is reflected most clearly in a Forward to the book "Spark Discharge," published by the Moscow Institute of Physics and Technology Press in 1997, a piece out of which appears below [11]. "*...We ventured to write it, believing that we know fairly much about the long spark. One of us investigated a spark discharge experimentally for thirty years, another tried to generalize and theoretically describe the accumulated data as far back as in the book "Gas Discharge Physics," where the largest chapter is devoted to a spark discharge. Alas, the self-reliance disappeared already in the very beginning of the work as soon as a primary spark element—an ionization wave (which is a streamer)—became the case in point. We have understood that the traditional consistent record of experimental data and theoretical constructs would hardly aid to present any whole picture of the discharge. It was obtained to be motley like a quilt,*

while among this diversity of colors, the naked holes gaped. ..."

Experimental studies of spark discharge show that dynamics of the electron-avalanche evolution is connected with the permanent change in the nature of interaction of the system charges, both with the external field and between each other. These are the interactions that predetermine a fate of the charge system. If the system density is low, then electrons and ions are almost independent and freely drift toward their electrodes. As the density of charges grows, the system begins to acquire the clearly pronounced non-equilibrium structure, and a linear behavior of the response of charges to an impact of the external field begins to break. We may suggest that if conditions, under which the charge system develops, contribute to intensification of its non-equilibrium state, then the system itself may become a cause of the ordered-structure formation. Such a cause in an electron avalanche is a volume (space) charge that grows with increase in the electron-avalanche density and has a great impact on the external electric field and the further fate of the avalanche.

A significant role of the space charge in the gas-charge evolution was indicated by K.K. Darrow in his book "Electrical Phenomena in Gases," published as early as 1936 [15]: "*The electric-field distortion is vitally required for a discharge. If we could find the prime cause of this effect, then we would understand the discharge phenomenon. The proximate cause, however, is clear: it is the presence of a space charge.*" Relying on this profound thought, it is possible to continue with certainty that *the avalanche-to-streamer transition is always accompanied with a strong distortion of the electric field by a space charge, which points at the existence of physical processes related to the very essence of the space charge owing to which this transition is implemented.*

At the Dzhelepov Laboratory of Nuclear Problems (DLNP) of the Joint Institute for Nuclear Research (JINR), while studying the operation of narrow-gap multiwire proportional chambers [16, 17] in the mode of high gas gain (10^7–10^8), previously unknown processes have been found that proceed in the dense heavy-current electron avalanche in the prestreamer region, namely: *change in the behavior of electron-avalanche evolution; the absence of induced charge on the chamber's cathode within the time of avalanche evolution; electrostatic oscillations of the completed avalanche; separation of the avalanche electrons according to velocities; different shapes of amplitude distributions of the signals, induced by the electron avalanche on the anode and cathode; shortening of the anode-signal duration; a high counting rate of* $5 \times 10^5\ c^{-1}\ \mathrm{cm}^{-2}$ *at the high gas gain* 5×10^7 [18, 19]. At the end of an operating range for high voltage, the chamber begins to transit to the streamer mode of operation, which is manifested in the jump of the anode pulse amplitude [20, 21]. The study and analysis of the indicated processes have led to the conclusion that they are, in essence, the attendant processes providing the electron avalanche-to-streamer transition and may be interpreted as a manifestation of properties of the double charge layer exposed to the external electric field [22].

The model [22] based on new experimental data is proposed by the author, making it possible to describe all processes related to the streamer formation and growth in both a strong external electric field and a weak one. The model describes a streamer structure and a cause of its stability; the mechanisms and causes of the ionization-wave emergence, the fast heating of ionized channel, and the increase in its electric conductivity are explained. Additionally, this model is well suited for solving problems which arise in studying long discharges, including a lightning discharge.

2. PRESSING PROBLEMS OF A LIGHTNING DISCHARGE

Studying processes of initiation, formation, and propagation of electrical discharges in air is of practical value, which encourages the development of experimental and theoretical methods for research of gas-discharge phenomena. However, the complicated spatial structure of lightning discharges and their weak luminosity in the fast-proceeding processes make their interpretation difficult. For clearer understanding of the physics of lightning, a number of questions are to be answered, most pressing of which are as follows: (i) what is the mechanism of gas heating in a streamer and a leader occurring for, literally, 10^{-8}–10^{-7} s (preventing thus the electrons from being captured by oxygen); (ii) how does a streamer grow in the weak electric field; (iii) what is the ionized-channel structure to be in order to ensure the channel stability; (iv) owing to what processes is the permanent heating of a growing leader causing the increase of its conductivity?

For solving the stated problems, the development of new approaches and obtainment of the new experimental results, which are capable of ensuring a major breakthrough in studying physics of spark discharge, are required.

2.1. Avalanche-to-Streamer Transition

By now the approach to explaining a transition of a single electron avalanche to a streamer has undergone large changes. However, according to prevalent conceptions, the preference is still given to the photon mechanism of streamer growing [11, 23–25] and the factors contributing to the avalanche-to-streamer transition are not considered. With photon mechanism of streamer growth, the possibility to achieve the critical number of electrons $(1–5) \times 10^8$ in the avalanche (on reaching which the avalanche-to-streamer transition occurs) is not explained. Moreover, the issue of how the stability is ensured in a plasma streamer is not considered.

The research [26] has shown that a short-wave radiation has the high absorption coefficient (μ = 200–600 cm^{-1}) and the relatively low yield of photons per a secondary electron ($N_{ph} \le 10^{-3}$ at $E/p \le$ 100 V/(cm Torr). With increase in the gas pressure, the number of photons N_{ph} decreases due to quenching of the excited atoms and molecules [8]. Moreover, the length of photon absorption in molecular gases is very small: ≈5–10 μm.

The fact that a process of streamer growth toward the cathode occurs—owing to the mechanism of photoionization—has a very modest experimental justification and is questioned permanently. If the process proceeds in complex gases, then a discharge occurs only at the single stage due to ionization by electron impact, while the influence of photon mechanism is completely eliminated. It is obvious that all this does not testify in favor of the mechanism of photoionization.

2.2. Ionization Wave

According to [11], in understanding a mechanism of emergence of an ionization wave, the problems arise concerning its propagation, the ionization rate and degree, i.e., the initial conductivity. Of particular difficulty is the issue of a radius of the plasma channel in the vicinity of its leading edge ("head" of the growing channel), with which the initial radius of the channel coincides. It is assumed that the processes, owing to which the certain (and in this case very small) mean radius is set, have been not quite clear so far. They, probably, go beyond the stationary processes of ionization, motion of charges, and formation of an electrostatic field in the region of developed ionization.

In addition, the very structure of ionized channel and processes occurring inside the channel is the unresolved problem. Now, there is no theory that would provide clear answers to all these questions. There are also no convincing experimental data which could clarify the understanding of the indicated processes [11].

2.3. Streamer Growth in a Weak Field

All streamer researchers are united in believing that a plasma channel, growing into a domain of the weak external field, creates for itself a field strong enough for ionization in the region of its leading edge (its "head"). However, the mechanism of creating a source of the strong field in the growing ionized channel is, in essence, of descriptive character and has not been clear until now [11].

2.4. Gas Temperature in the Channel

The issue of gas temperature in the growing plasma channel has a cardinal importance for solving the problems related to a spark breakdown in air. In the cold air, in the absence of sufficiently strong field, the electrons live not very long because of their adhesion to oxygen. With the adhesion rate $\nu_a \approx 10^7$–10^8 s^{-1} and the ionization-wave velocity $v_c \approx 10^8$–10^9 cm/s, the plasma conductivity has to sharply decrease at distances of the order of 10–100 cm behind the ionization-wave front [11]. Meanwhile, a spark breakdown of many-meter air gaps is quite attainable, it is observed and investigated in experiment, as is lightning when the high-conductive ionized channel covers a few kilometers. This is possible only at the gas temperature no less than 3000°C, when the processes of electron detachment hinder a rapid degrease in conductivity [11, 12].

According to assessments performed in [12], the amount of energy (released in 1 cm^3 for 1 s as a result of passage of the ionization wave and the streamer current) is roughly 5×10^{-3} J/cm^3. It is evident that these currents are incapable of resolving the problem of high-temperature gas heating.

It is believed in [12] that currents of all streamers that represent the streamer crown and are linked to the their start point (leader-channel head) heat up this region by combining together and contribute to the leader advance over a distance equal to the radius of leader head. From this it follows, as the authors believe, that a leader current is a sum of numerous (but very weak) streamer currents. If the leader moves forward a radius of its "head" amounting to roughly 3–5 cm, then it is unclear for what purpose the streamers with a mean length of 50 m are formed in the streamer zone.

As we can see, there is no reasonable mechanism explaining the gas heating in the fast-proceeding processes of growth of a streamer and a leader.

2.5. Streamer-to-Leader Transition

According to the authors of [11], a streamer-to-leader transition is most difficult for the theory, poorly studied, and even not completely understood in many respects; at the same time, it is one of the most important stages of the leader process.

2.6. Conductivity of a Lightning Channel

A lightning channel is discharged at the time of the main stroke at a rate of $(0.3–0.5) \times 10^{10}$ cm/s, which is more than 100 times higher than the leader rate at which the lightning channel was charged during its growth. From this it follows that the channel is discharged with the 10^2–10^3 times higher current than the leader current (≈100 A). Accordingly, approximately in the same ratio, the channel's resistance per unit length R_0 also decreases during the transition from charging to discharge [12]. The channel heating during the heavy current passage, due to which the plasma conductivity increases, is considered to be a reason for decrease in the resistance.

The initial leader channel with high resistance can pass current within the limits of ≈100 A [12]. In order

for the ionized channel to be capable of passing currents with the amplitude of a few tens and hundreds of kiloamperes, a total ohmic resistance of the entire channel with a length of a few kilometers has to be no more than 10^2 Ω [12]. However, this may take place only after heating of the ionized channel up to temperatures of the order of (20000–35000)°C. The entire ionized channel has to be heated, and it takes some time; therefore the heating process cannot occur simultaneously with onset of flowing of the large-amplitude current through the channel. Thus, the issue of dynamics of change in the resistance of lightning channel remains open.

2.7. Coherent Radiation of the Return Stroke of Lightning

On August 20, 1999, a group of researchers from the Moscow Institute of Physics and Technology using the pulse radiometric complex recorded a coherent microwave signal from the initial stage of the lightning return stroke, beginning from the moment when the stepped leader overlapped the gap between the cloud and the ground [27]. The signal was found to be complex, consisting of a series of single pulses with the duration in excess of 5 μs, partly superimposed on each other. The total duration was 60 μs. The repeated measurement of this process, which completely confirmed the previous result, was performed by the same group in 2011 [28]. Until now, no explanation has been offered for the observed phenomenon.

2.8. Neutron Production in a Lightning Discharge

The first experimental indication of the neutron production under lightning activity was obtained in 1985. Today this phenomenon continues to be detected by the contemporary ground-based installations. A.V. Gurevich with his co-authors [29] reported on detection of thermal neutrons during the lightning discharges at the Tien Shan Mountain Station. The neutron flux in almost direct proximity to the lightning was found to be ≈5000 $n/(m^3\ s)$. However, this value may be slightly overestimated due to the γ-radiation detected by neutron detectors, which, in correlation with thunderstorms, is created within a wide energy range.

In the modern view, neutrons are produced in the thunderstorm atmosphere as a result of photonuclear reactions, or conditions may appear in the lightning channel which are sufficient for initiation of the fusion reaction with participation of deuterium contained in water vapors, i.e., $d + d = {}^3\mathrm{He} + n + 3.28$ MeV [30].

A version of fusion seems to be logical, but here, as is considered, due to a low cross section of the ${}^2\mathrm{H}({}^2\mathrm{H}, n){}^3\mathrm{He}$ reaction ($\sigma_{fus} = 10^{-36}$–10^{-32} m), a fusion reaction is absolutely impossible under conditions implemented in the lightning channel according to the modern ideas [31–33]. As distinct from the nuclear fusion, the authors of [33] believe that photonuclear reactions can be responsible for the probable enhancement in a neutron flux in the thunderstorm atmosphere because, in correlation with thunderstorms, the γ-radiation bursts have been repeatedly detected with the energies $E_\gamma \geq 10$ MeV that is above the threshold of photonuclear reactions in air.

Despite the fairly old history of observations and the substantial number of theoretical works devoted to the mechanism of neutron production during the thunderstorm activity, an issue of origin of these neutrons remains open.

2.9. Lightning Protection

According to statistics, 40000 thunderstorms occur daily in the world, 117 lightning flashes happen every second. Suffice it to say that more than 3000 people per year die in the world from lightning strikes (which is more than the number of people killed in plane crashes), while a material damage is counted by billions of dollars. Large human and economic losses caused by destructive activities of lightning discharges are related first of all to a low efficiency of the used lightning conductors ($\epsilon \approx 20$–25%). The photographs given in Fig. 1 are vivid evidence of it: lightning has struck the Eiffel Tower up to 100 m below the spire. The same situation is observed with the Ostankinskaya television tower (Fig. 1b). *The majority of downward lightnings overshot a substantial distance, not getting on the tip of the lightning rod. It is a very serious argument against the well-spread explanation of the main operating principle of lightning conductors: a rod "attracts" lightning* [12].

To increase the efficiency of lightning conductors, attempts were made to drive a counter leader growing from the ground at maximum possible speed. To succeed, the amplitude of control action for initiating the leader must be a few hundreds of kilovolts, which is technically difficult and requires great financial costs.

The produced modern lightning conductors of early streamer emission (ESE) surpass in nothing the widely used lightning conductors of the rod type.

2.10. Ball Lightning

Ball lightning is a phenomenon of natural electricity: a glowing sphere that travels along the unpredictable path and has many other mysterious properties. To this very day, ball lightning has not been produced under laboratory conditions and remains to be the insufficiently explored phenomenon, offering a ground for speculations. There are hundreds of versions of ball-lightning origin [34], in which the authors largely try to reconstruct it instead of providing the simple and clear explanation of its properties and a mechanism of formation. In order not to remain aloof from the popular and mysterious problem, we propose

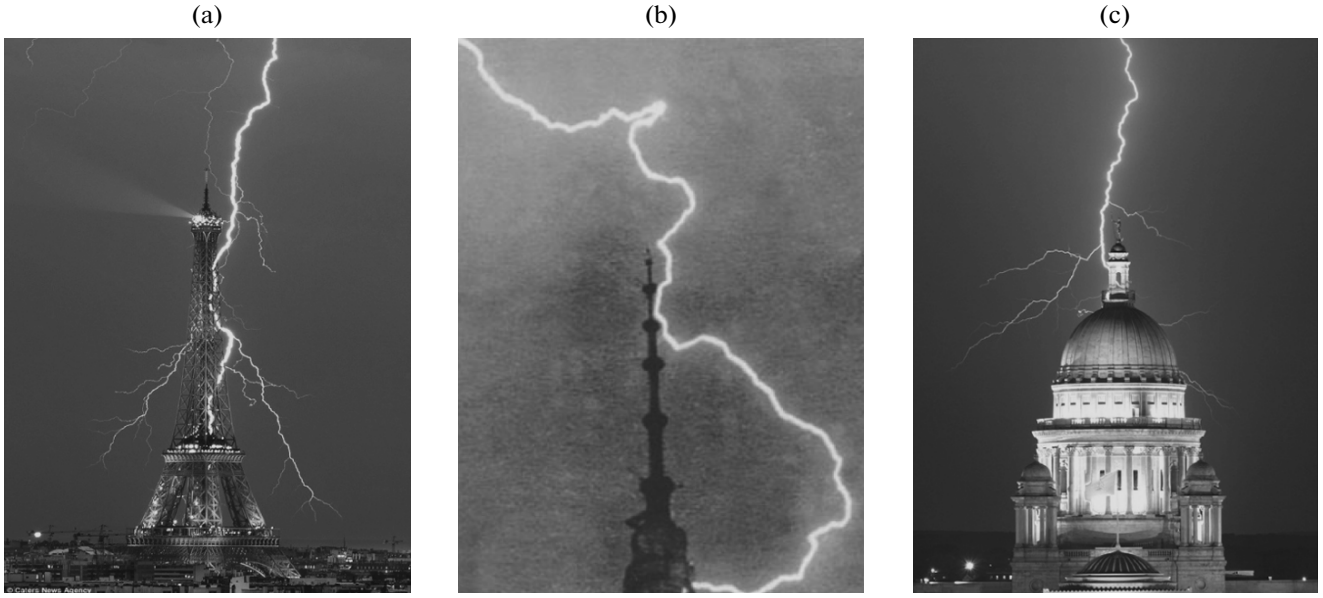

Fig. 1. The lightning has struck below the spire of: (a) the Eiffel Tower (by 100 m); (b) the Ostankinskaya Tower (by 200 m); (c) the building (by 20 m).

in this work (section 3.8) one more variant of the mechanism of ball-lightning formation.

3. DYNAMICS OF THE STREAMER FORMATION

At the JINR DLNP, while studying the operation of narrow-gap multiwire proportional chambers [16, 17] in the gas-gain interval of $\leq 10^8$, previously unknown processes were found that occur in the dense heavy-current electron avalanche within the pre-streamer region: *a change in the character of electron-avalanche development; the absence of induced charge on the chamber cathode during the time of avalanche evolution; electrostatic oscillations of the avalanche completed as a whole; velocity separation of the avalanche electrons; different shapes of amplitude distributions of signals induced by the electron avalanche on the anode and cathode; shortening of the anode-signal duration; a counting rate of the chamber with the gas multiplication factor* $M = 10^7$–5×10^7 *is* 5×10^5 s^{-1} cm^{-2} [18, 19]. At the end of the operating range for high voltage (in a gas-gain interval of 5×10^7–10^8), the transition to the streamer operating mode of the chamber starts, which is expressed in the amplitude jump [20, 21].

Information on the processes occurring in the electron avalanche is obtained in the chamber with an anode wire pitch of 1 mm and the anode–cathode gap of 1.5 mm. A diameter of anode wires is 20 μm. A working high-voltage plateau in the chamber was 1600 V, which provided the possibility of chamber operation in one of four modes: the proportional mode, the limited proportionality mode, the plasma streamer mode, and the self-quenching streamer mode. Measurements were taken at the test bench (Fig. 2) with the use of radioactive sources ^{90}Sr and ^{55}Fe. A high voltage was supplied to the cathodes through the 3-MΩ resistor. Information was picked off the cathodes through a 220 pF × 6 kV capacitor.

A passage of β particles through the chamber was detected by the scintillation counter, which was viewed from its edges by two photomultiplier tubes (PMTs) connected to a coincidence circuit. Signals from the coincidence circuits were used for synchronization of the oscilloscope, for control of the Charge-Code unit while analyzing amplitude characteristics, and as a Start signal while measuring the chamber's time characteristics. The electron beam and its intensity were formed using the regulated slit collimators installed before the chamber and directly on the scintillation counter.

In the logic of separating an event of electron passage through the chamber (see Fig. 2), a single anode wire 2, connected to the coincidence circuit with the scintillation counter, was used. A synchronizing signal for the oscilloscope was generated by the coincidence circuit on arrival of a signal from wire 2. This made it possible to fix a position of signals from the chamber on the oscilloscope sweep. The induced signals from the combined anode wires 1 and 3 (performing a role of check wires), from the combined cathode planes, and from the anode wire 2 were subject to analysis. The signals from wires 1 and 3 were measured simultaneously with either cathode or anode signals. The time of propagation of signals from the chamber electrodes to the oscilloscope input was 50 ± 0.1 ns. Measurements were conducted using the TDS 380 digital dou-

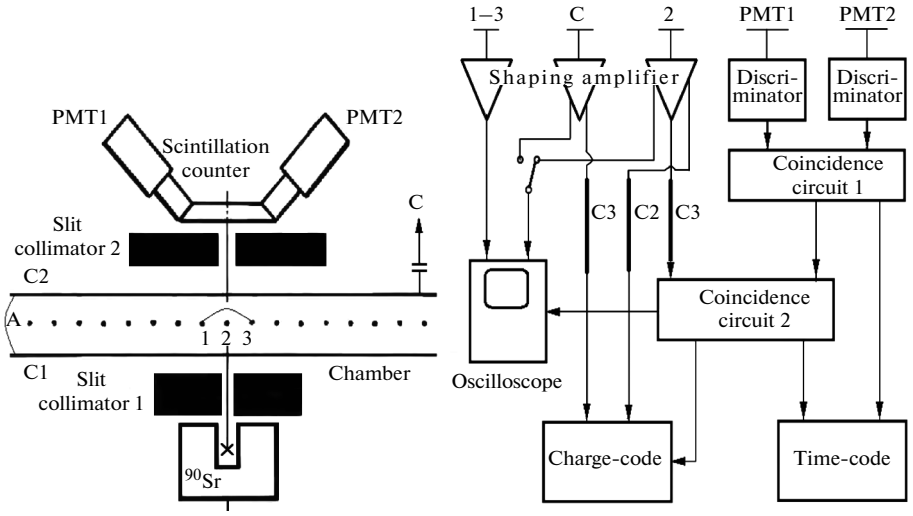

Fig. 2. Block-diagram of measuring the characteristics of electron avalanche.

ble-trace oscilloscope. Information about the electron-avalanche behavior in six different gas mixtures depending on the chamber high voltage is given in [18, 19].

Below, a brief description of some physical processes which provide the electron avalanche-to-streamer transition is given. A lack of induced charge on the chamber cathode during the time of the electron-avalanche evolution in the "heavy" gas (80% CF_4 + 20% C_4H_{10}) is related to the fact that a bulk of electrons in the avalanche is slow [35]. Ions and electrons overlap and drift in opposite directions. With the sufficient avalanche density, the drift will lead to emergence of the polarization field induced by separation of charges, which is equivalent to a certain dipole with charges $N_e \approx N_i$, located at a distance of the ionization length α^{-1} (Fig. 3) [11]. The external field E_0 at the dipole

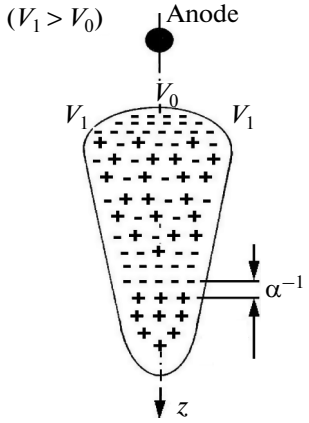

Fig. 3. Charge distribution in the avalanche during the dipole formation.

center will weaken down to zero when the field, created in it by the electron and ion charges separately, $E_1 = eN_e \cdot 4\alpha^2/(4\pi\epsilon_0)$, reaches the value $E_0/2$. It will happen when the number of electrons in the avalanche grows up to the critical value $N_{cr} = \pi\epsilon_0 E_0/(2e\alpha^2)$ [11].

Based on the equality $E_0 = 2E_1$, we express the external field strength through the avalanche density n_e by presenting the polarization field as $E_1 = 4\pi e n_e \alpha^{-1}/(4\pi\epsilon_0)$ [36]:

$$E_0 = 2E_1 = 2 \cdot \frac{4\pi e n_e \alpha^{-1}}{4\pi\epsilon_0} = 2 \cdot \frac{e n_e \alpha^{-1}}{\epsilon_0}. \quad (1)$$

After substitution of the expression for E_0 into N_{cr}, we derive "*the constant*" [18], which is a criterion for the dipole formation, i.e., a ratio of the electron density in the avalanche to a cube of the ionization coefficient, at which this density has been reached, which is always equal to the critical number of electrons

$$N_{cr} = \pi \cdot \frac{n_e}{\alpha^3}, \text{ or } \alpha = \left(\pi \cdot \frac{n_e}{N_{cr}}\right)^{1/3} = \sqrt[3]{\frac{\pi}{N_{cr}}} \cdot \sqrt[3]{n_e} = 5.4 \times 10^{-2} \cdot \sqrt[3]{n_e}. \quad (2)$$

A link of the first Townsend coefficient with the avalanche density reflects the electron-avalanche evolution in space and can be used for theoretical calculations and estimations. In the narrow-gap chamber with gas filling of 80%CF_4 + 20%C_4H_{10}, we obtain $N_{cr} \approx 2 \times 10^4$ [19]. Thus, starting from the instant when the equality of the charge-separation field and the external field is established, in a tail of the evolving avalanche, an immobile dipole forms in which the ions shield the cathode from the electrons moving toward the anode.

Since the drift current is absent for the time of the cathode signal delay (2–3 ns) [19], the power supply does not do the work for separating charges over this period of time. **As a result, electrons and ions overlap, which leads to the field attenuation in the avalanche bulk and it transforms to the plasma formation.** A low field and a high density gradient in the avalanche will induce a diffusion of electrons in the direction of strong fields and low density, i.e., toward the region around the center of gravity of the electrons in the avalanche head. Eventually, the diffusion of electrons will lead to the electron-avalanche expansion that is called the Coulomb repulsion of charges [10, 23].

Despite the absence of drift current in the chamber simultaneously with the diffusion, the electron avalanche continues to evolve in the field created between the electrons and the charges on the anode as a result of electrostatic induction. Ionization is produced due to the energy stored in the anode-wire capacitance with respect to the ground. Because the charge density in this region grows sharply, a substantial space charge forms due to the diffusion of electrons into the avalanche head and the charge separation. The space-charge growth restrains the diffusing electrons, and owing to ambipolar diffusion, the electrons will pull the ions to the last ionic layer. The increase in the space charge will lead not only to the substantial growth in the field between the frontal electrons and the ionic layer but also to termination of the electron avalanche [19].

The termination of avalanche evolution far from the anode serves as the explanation of the high radiation resistance of narrow-gap chambers filled with a gas mixture of 80% CF_4 + 20% C_4H_{10}. Despite the chamber operation under exposure to intense fluxes of charged particles (10^7–10^8 s^{-1} cm^{-2}) and the large content of isobutane (20%)—which is a source of radicals contaminating the anode wires 20 μm in diameter—the detection characteristics of the chambers were maintained after a passage of 3×10^{13} particles/cm^2 through them [37, 38], which exceeds by approximately a factor of 100 the radiation resistance of standard chambers [39], in which the avalanche terminates on the surface of anode wires.

Eventually, the main part of electrons and ions diffuses into a peripheral region of avalanche head, and the avalanche head transforms to the polarized charge bunch (Fig. 4). The diffusion-induced redistribution of electrons will cause the diffusion current. Flowing through the load resistor of the triggered anode wire 2, the diffusion current will branch out via the ground bus over the rest of anode wires of the chamber and will close on the frontal layer of the avalanche electrons through the input resistors of amplifiers and partial capacitors (capacitive coefficients) [41] between the wires and the avalanche. For the time of exposure to the diffusion current (roughly 2–3 ns), the electron avalanche, by undergoing the diffusion expansion,

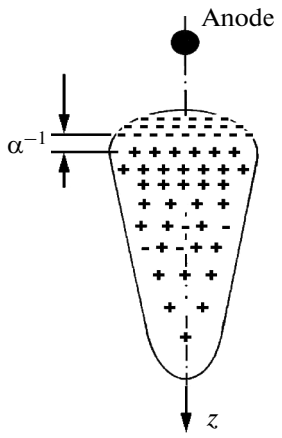

Fig. 4. Schematic outline of the charge distribution in the avalanche by the moment of termination of diffusion current.

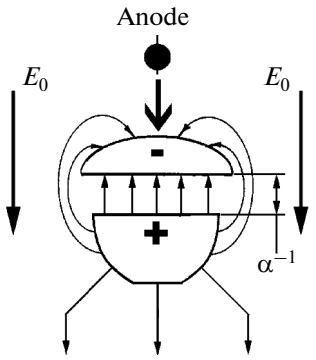

Fig. 5. Electric field lines in the region of double layer.

transforms to a double charge layer, as is shown in Fig. 5. Formation of the double charge layer will cause a jump in potential on the ionic layer, which, after summing up with the potential created by a power supply in this region, will lead to an increase in the field behind the positive layer. With transition of electrons from the avalanche bulk into its head, the growing field of ions will destruct the dipole structure in the avalanche tail. A graphic illustration of the region of location of charge layers with respect to the anode wire on the potential-distribution curve (within the limits of 0.004 cm from the anode axis) is given in Fig. 6.

For determination of the further behavior of the created charge system, we proceed from the assumption that an electric field in the vicinity of the formed charge layers is inhomogeneous. Let the field strength be $\mathbf{E}(\mathbf{x}_-)$ at the center of gravity of the negative layer and $\mathbf{E}(\mathbf{x}_-) + \Delta\mathbf{E}$ at the center of gravity of the positive surface, where $\Delta\mathbf{E}$ is the field increment caused by the potential jump. Then the double charge layer will be

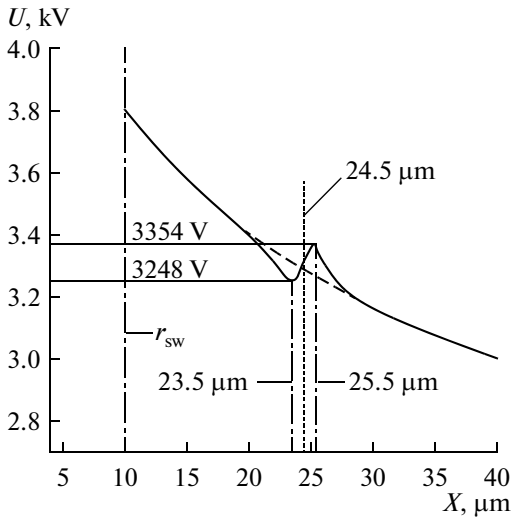

Fig. 6. Potential distribution in the region of formation of the double charge layer.

exposed to the force induced by the inhomogeneous enhanced field and directed toward the cathode:

$$\mathbf{F}_{xC} = (N_i - N_e)e\mathbf{E}(\mathbf{x}_-) + N_i e\alpha_0^{-1}\frac{\mathbf{\Delta E}}{\alpha_0^{-1}} = (N_i - N_e)e\mathbf{E}(\mathbf{x}_-) + N_i e\alpha_0^{-1}\frac{\partial \mathbf{E}(\mathbf{x}_+)}{\partial\alpha}, \quad (3)$$

where $\partial\mathbf{E}(\mathbf{x}_+)/\partial\alpha$ is the derivative of the E vector in the α direction coinciding with the direction of the $\mathbf{E}$ vector increment. From Eq. (3) it follows that the double layer that is coupled to its intrinsic field and exposed to the inhomogeneous electric field undergoes the force action from the field and is drawn into the region of the stronger field, i.e., should start moving in the direction of the cathode. A motion of the double charge layer toward the cathode along the decreasing external field will weaken an action of the driving force (3). In this case, the restoring force from the anode increases. Acting from the charge system, the force will add some acceleration to it and restore it to the initial position. Owing to the inertia, the charge system will miss the initial position. Then everything will be repeated, and the double charge layer will change to the oscillating motion along the external field direction.

In [18, 19], the oscillograms measured in the case of filling the chamber with six different gas mixtures are given. From the oscillograms it can be seen that the amplitude and duration of oscillations depend to a different degree upon the gas-mixture composition and the gas gain in the chamber. From comparing the oscillograms it follows that the denser the avalanche is, the stronger the manifestation of oscillating processes in it, and the higher their frequencies. In the gas mixtures 70% Ar + 30% C_4H_{10} and 95% CF_4 + 5% C_4H_{10}, the oscillations very weakly reveal themselves only at the end of the chamber's operating range for high voltage. It is explained by a low density of the electron avalanche for the former gas composition. The latter gas mixture with CF_4, whose purity is 99.7%, includes electronegative impurities (Freon 12 and Freon 13), while isobutane plays a role of the "quenching" additive, which reduces the thermal energy of electrons in the avalanche, by which the electron capture weakens [41]. Therefore, with a decrease in isobutane in the gas mixture, the "quenching" effect attenuates, and a part of electrons is absorbed by weakening the electron avalanche.

Let us note that the observed oscillations are not associated with the avalanche-induced shock excitation of the natural oscillations of the inductive-capacitive system of the chamber. Otherwise, oscillations at different electrodes must have the same phase, while in the chambers, having different pitch and anode diameter, different oscillation frequencies would be observed. If the avalanche loop, connected to the charged system of the chamber's electrodes through partial capacitors [40], were a source of the detected oscillations, then different frequencies would be observed in different chambers due to the more than double difference in the distributed parameters of the chambers. The observed oscillations do not result from a mismatch between the chamber's wave impedance and the input impedance of the oscilloscope and linear fan-out since a change in the matching impedance on the anodes has no impact on the oscillation frequency. Finally, the oscillations are not related to transients at the input of the oscilloscope amplifiers, since when the signals with the same amplitude obtained in different gas mixtures are detected, the absence or presence of oscillations are observed.

Figure 7 presents the (superimposed on each other) oscillograms measured on the anode, cathode, and check wires in the gas mixture 85% CF_4 + 13% C_4H_{10} + 2% $CO(CH_3)_2$ at the chamber high voltage of 3.2 kV [19]. The figure displays a change in the shape of signals caused by the joint oscillations of charges, a value of the cathode-pulse delay relative to the anode pulse, as well as the equality of oscillation phases of charge layers. A frequency and a phase of signals from check wires (upper oscillogram) coincide. It can be clearly seen that oscillation frequencies of the anode and cathode signals coincide. A direction of motion of the double layer during its oscillations is determined from the polarity of signals induced by the electron and ionic layers at the anode and cathode, respectively. In motion toward the cathode, the cathode signal amplitude grows while the anode signal duration becomes shorter. At last, it can be seen that the cathode signal arises after the anode signal reaches half maximum of its peak value.

As an example, we give some experimental data which result from the presence of the double charge layer and its oscillations.

Counting rate of high-speed narrow-gap chambers. According to assessments performed in [42], the impact of space charge on the external field in the region of avalanche formation will be of the order of 2–3% if, in the course chamber irradiation by the beam with a density of 10^7 s^{-1} cm^{-2}, ions displace from the avalanche-formation region toward the cathode by 100 μm for time smaller than the duration of intervals between the beam particles. From this constraint it follows that a drift velocity of ions has to be $\geq 10^5$ cm/s. However, in the domain of the reduced electric field E/p = 90–300 V/(cm Torr), the drift velocity of ions for the chambers under study, according to the approximation $v_i = bE/p$ (where b = 175), is equal to $v_i \approx 3 \times 10^4$ cm/s [23]. At this velocity, the ions will drift a distance of 100 μm for 330 ns. This value of drift time of the ions substantially exceeds the mean time interval between particles of the beam with a density of 10^7 s^{-1} cm^{-2}, which (being of statistical nature) may change to become either higher or lower.

At the same time, the operation of narrow-gap chambers in intense particle fluxes has demonstrated their high counting rate. For example, according to the studies carried out by the team of J. Fischer [41] on test chambers for very high counting rates at a gas gain of $\approx 6 \times 10^4$, it was found that in the chamber with an anode wire pitch of 1.27 mm, an anode-to-cathode gap of 1 mm, and the anode wire diameter d_a = 10 μm, the amplitude on the anode drops by 10% at an intensity of 10^7 s^{-1} cm^{-2} and by 16% at an intensity of 2×10^7 s^{-1} cm^{-2}. At the same time, for a chamber with an anode wire pitch of 0.79 mm, the anode-to-cathode distance 0.635 mm, and d_a = 8 μm, no impact of the space charge was observed up to loads of 10^8 s^{-1} cm^{-2}. With a low gas gain, the amount of ions in the avalanche is small. In the intense fluxes, however, ions should accumulate in the anode region due to the relatively low drift velocity. However, this is not observed.

In our measurements at relatively high gas gain ($\approx 3.5 \times 10^5$) in the chambers with an anode wire pitch of 1 mm, an anode-to-cathode distance of 1.5 mm, and d_a = 20 μm, chamber efficiency dropped from 99.6% to 98% only at the intensity 10^7 s^{-1} cm^{-2} [38]. From these data it follows that the responsibility for fast evacuation of ions from the avalanche region toward the cathode does not rest with the drift velocity: another mechanism is responsible, due to which the ions leave for the cathode from the avalanche region by covering a significant distance in a few nanoseconds. This mechanism is the process of oscillations of the charge system of the avalanche, as a result of which the ions of space charge evacuate during 2 ns in the direction of the cathode over the distance equal to the oscillation amplitude, i.e., 200 μm.

It should be added that a displacement of the double charge layer toward the cathode at an oscillation velocity $u_i \approx 10^7$ cm/s and a fast decay of oscillations allow a counting rate of 5×10^5 s^{-1} cm^{-2} to be achieved

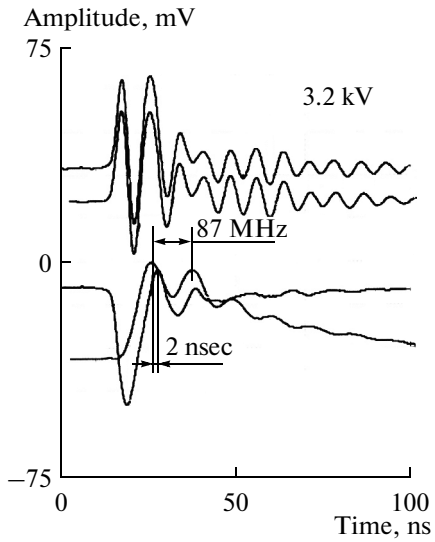

Fig. 7. Oscillograms of joint oscillations of the electron and ionic layers. The gas filling of the chamber: 85% CF_4 + 13% C_4H_{10} + 2% $CO(CH_3)_2$. Attenuation of the anode and cathode signals is 10 dB.

in the mode of large gas gain (10^7–5×10^7). With the comparable characteristics of currents, a counting rate of the chamber that operates in the plasma mode is more than two orders of magnitude higher than the counting rate achieved in the self-quenching streamer mode. In addition, chambers that operate in plasma mode have an order of magnitude higher radiation resistance.

Shortening of duration of anode signals. With increase in the gas gain, a gradual shortening of anode signal duration is observed in the narrow-gap chamber (Fig. 8). If in the proportional mode, the full pulse duration is ≈30 ns, then in the heavy-current mode, the signal duration decreases down to 5–10 ns depending on gas filling of the chamber [18, 19]. Shortening of the anode signal duration is related to the superposition (on its trailing edge) of the inverse-polarity signal induced during the half-period on the anode while electrons are traveling to the cathode as a result of the charge-system oscillations. We note that as a result of summing the different-polarity signals, a slow ionic component that is inherent in current signals from the electron avalanche in a strongly inhomogeneous field completely vanishes.

For additional confirmation of the effect of shortening of anode signals induced by oscillations of the double charge layer, a photograph of the anode signal from the avalanche in the gas mixture 80% CF_4 + 20% C_4H_{10} at a high voltage of ≥3700 V is given in Fig. 9 (photo 1). A similar situation is found in operation of chambers, which were investigated by the team of G. Charpak [43], as well as during the operation of proportional tubes with small diameter filled with xenon [44]. Figure 9 (photos 2 and 3) presents for

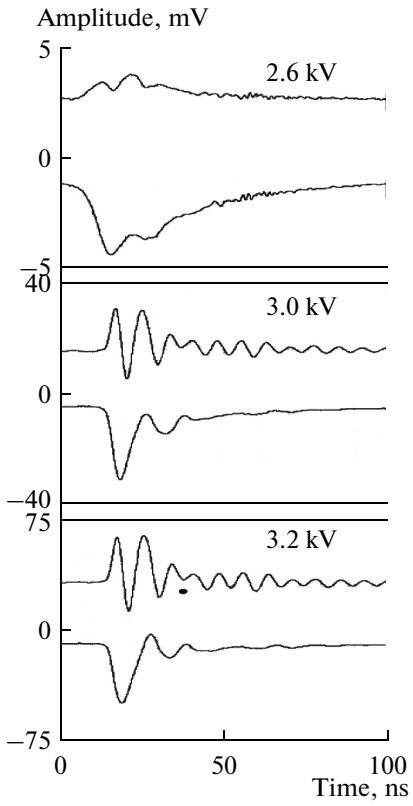

Fig. 8. Shortening of the anode pulse duration (lower oscillograms) caused by the avalanche oscillations in the gas mixture 90% CF_4 + 9.88% C_4H_{10} + 0.12% Hg. The chamber high voltage is indicated on oscillograms. Attenuation of anode signals is 10 dB.

comparison the photographs of signals borrowed from [43], where a contribution of the slow ionic component to the signal duration is absent and the clearly pronounced oscillating processes in the avalanche are shown.

Separation of electrons according to velocities. Since there is no drift current within the delay time of cathode signal (2–3 ns) [19], then a power supply does no work on charge separation during this time. As a result, electrons and ions overlap each other, which leads to the field attenuation in the bulk of the avalanche, and so it transforms to a plasma formation. Under these conditions, due to a lack of retarding forces from the ions, the electrons residing at the front of the plasma formation may transit to the mode of weak acceleration.

For example, time spectra measured at different high voltages are given in Fig. 10. The time spectrum of signals from the anode of chamber 1, obtained at the voltage of 2300 V, is well described by a Gaussian distribution and indicates that the electron distribution in velocities approaches the Maxwellian one. Distribution 2, obtained at the voltage of 3700 V, shows the evident violation of the Maxwellian distribution and points to the presence of two electron groups in the

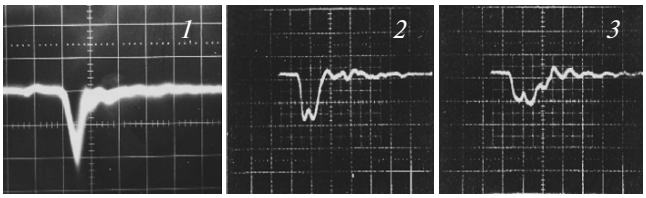

Fig. 9. Photographs of signals from the oscilloscope screen arriving directly from the anode wire of the chamber: (*1*) sweep 5 ns/cm; sensitivity 100 mV/cm; U_{ch} = 3700 V; (*2*, *3*) sweep 5 ns/cm; sensitivity 20 mV/cm; of the chamber is filled with pentane gas; U_{ch} = 4000 V. Photographs 2 and 3 are taken from [43].

avalanche: fast and slow electrons. Separation of electrons according to velocities begins to manifest itself in the time spectra at a voltage of 2900 V and intensifies as the voltage increases.

A fraction of fast electrons contained in spectrum *2* (Fig. 10a) may be determined if the spectrum is presented as a sum of two spectra described by a Gaussian distribution. This operation is shown in Fig. 10a, from which it can be seen that the number of fast electrons is ≈30% of their total amount in the avalanche.

Different shapes of amplitude spectra measured on the chamber's anode and cathode. Since the opposite charges are coupled to the intrinsic field, the motion of electrons is shielded from the cathode by the ionic layer, while the motion of ions is screened from the anode by the electron layer. At this stage, a change in signals on the anode and cathode is mainly caused by bias currents flowing in the chamber, which are induced by polarization of the electrodes exposed to the varying electric field of oscillating charges. The approach of ions of the polarized bunch to the cathode in the process of oscillations induces on it the negative charge that is 30% more than the electron-induced charge on the anode because 30% comprising "fast" electrons, as has been mentioned in section 3.5, have gone to the anode [18]. The faster growth in the cathode signals, as compared to the anode signals, with an increase in the high voltage is well confirmed by the amplitude spectra measured on the anode and cathode at the voltage of 3.8 kV (Fig. 11). A ratio of mean amplitudes of the anode and cathode signals is 1.6, whereas in the proportional mode, this ratio is more than 3. Thus, the currents responsible for signal formation on the chamber electrodes (diffusion current, fast-electrons current, and bias currents), due to the peculiarities of their flowing through the chamber and the external circuit, lead to different shapes of signals on the anode and cathode.

According to the theory of oscillations, oscillations of the system, bound with elastic forces, are characterized by the coefficient of association [45]:

$$\sigma = \gamma_2 \frac{2n_1 n_2}{\left|n_1^2 - n_2^2\right|}. \quad (4)$$

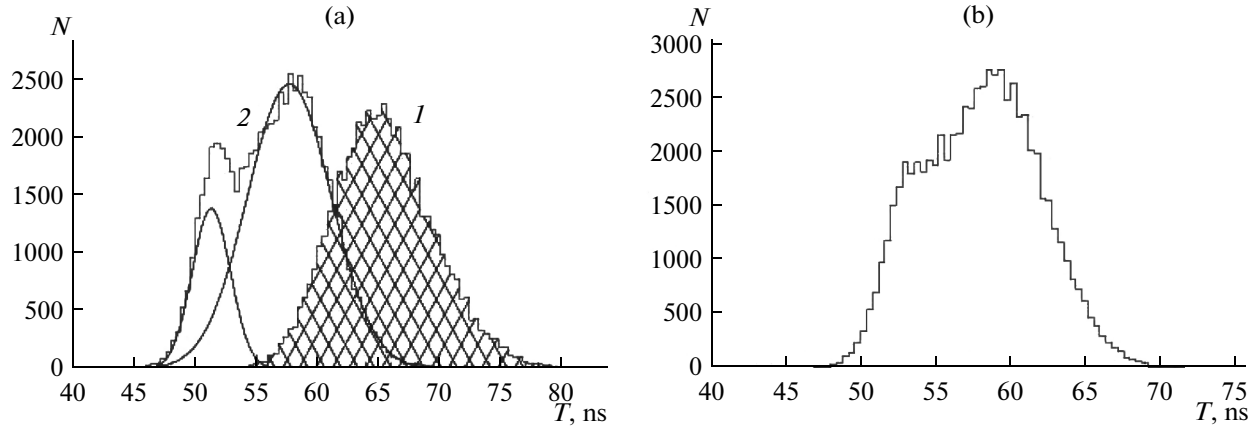

Fig. 10. Time spectrum of signals from the chamber anode at different voltages.

The coherence of two systems is that a nature of interaction between the systems is determined not only by a value of binding forces (γ_2) but also a proximity of partial frequencies (n_1, n_2) to each other. If the value $\sigma \ll 1$ (but not γ_2), then the interaction between the systems is weak, the *connectivity* is too small. With $n_1 \to n_2$, the coefficient of connectivity increases significantly even with small values of binding forces (γ_2), i.e., small binding forces have a substantial influence on the processes if partial frequencies are close to each other. In these cases, the parts of the coupled system oscillate at the same frequencies. On the contrary, with the substantial difference in partial frequencies, even relatively large binding forces make no difference to oscillations of each individual system.

In our case, oscillations of the polarized charge system with two degrees-of-freedom are also characterized by two oscillation modes [45]. At the high voltage U_{ch} = 3–3.4 kV (gas gain $\leq 5 \times 10^7$), the polarized charge system has the relatively low density ($\leq 10^{13}$ cm^{-3}). A resulting field near the ionic layer will be less than the field inside the "double" layer [22[. In this case, the bound charges oscillate at the same frequency as if the driving and restoring forces were less than a force of attraction between the layers. Then a coupling between the charge surfaces is sufficient for joint oscillations to occur in the same phase (see Fig. 7). After approximately 100–150 ns, due to the lack of energy inflow and collisions of charges with neutral atoms, the oscillations decay. This situation is achieved within a range of voltages of 400 V and can be clearly seen in Fig. 11a and Fig. 12 taken from [19].

With the gain growth to 10^8 (U_{ch} = 3.3–3.7 kV), the field on the anode side of the double layer will decrease more slowly than the field will increase on the side of cathode, since, due to a small distance between the layers, roughly 30% ions, by closing to electrons on the anode side (the number of electrons is 30% less than the number of ions, see below), will enhance the field in this domain (see Fig. 5). As a result, the force that retains the electrons grows. The deceleration of electrons is accompanied by diffusion. A reduction in the density of the electron layer will reduce the field between the layers, which will enable the ionic layer to break away from the electron layer under exposure to the driving force (3) and to begin the accelerated motion toward the cathode. Eventually, the second mode of oscillations will begin to manifest itself in the oscillating system. It is connected with the relative motion of oscillating surfaces of the double layer and will determine the further fate of the discharge development.

The above described oscillations are self-excited oscillations because the periodic movements arise in the absence of an external periodic action. A nature of oscillations is determined by the position of the double charge layer in the inhomogeneous electric field which, by compensating for energy loss during the oscillations, is the inherent part of the oscillating system. And the

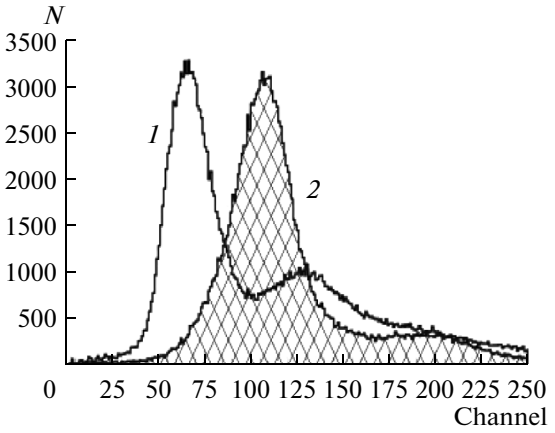

Fig. 11. Amplitude distribution of signals measured with the gas mixture 83% CF_4 + 17% C_4H_{10}: (*1*) spectrum of cathode signals; (*2*) spectrum of anode signals; 3800 V, attenuation is (*1*) 40 dB, (*2*) 40 dB.

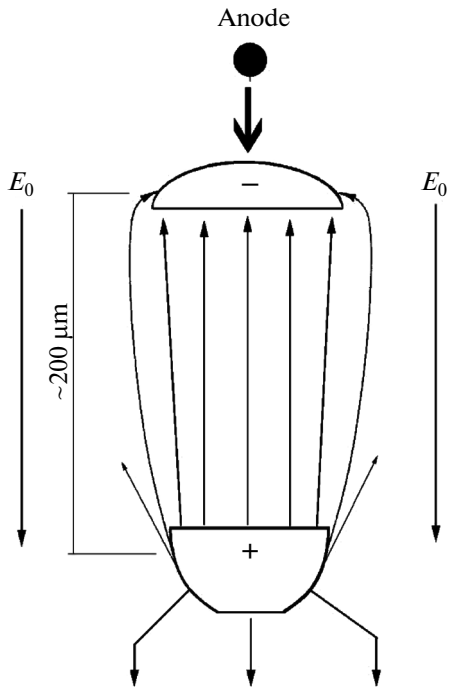

Fig. 12. Electric field lines after displacement of ions toward the cathode.

most important thing is that the self-oscillating systems are nonlinear systems in principle [45].

Oscillations presented in Fig. 7 are close to sinusoidal oscillations. Therefore for evaluation of the oscillating velocity and the amplitude of displacement of the double charge layer, the expressions used for definition of parameters of charge oscillations in the oscillating field can be applied:

$$u_e = \frac{eE_1}{m\omega_e} \approx 6.8 \times 10^8 \text{ cm/s},$$
$$a_e = \frac{eE_1}{m\omega_e^2} = 5 \times 10^{-4} \text{ cm}, \quad (5)$$

where $E_1 = 5.4 \times 10^5$ V/cm is the strength of electric field of charge separation on the length α_0^{-1}. The frequency of joint oscillations of ions and electrons $\omega = 2\pi f = 5.46 \times 10^8$ s^{-1} is determined from graphs in Fig. 7. The oscillating velocity and the amplitude of displacement of ions and electrons will be $u_i \approx 1.05 \times 10^7$ cm/s; $a_i \approx 1.93 \times 10^{-2}$ cm. Thus, the electrons simultaneously participate in two oscillating movements: natural plasma oscillations ($n_e = 5.7 \times 10^{14}$ cm^{-3}, $\omega_e = (4\pi n_e e^2/m)^{1/2} = 13.5 \times 10^{11}$ s^{-1}) and joint oscillations with ions.

The ions with the oscillation velocity 10^7 cm/s will displace roughly a value of the oscillation amplitude $x = 2 \times 10^{-2}$ cm toward the cathode [19, 22]. The motion of ions to the cathode at a high oscillating velocity will lead to a sharp rise in the current that testifies to the onset of the streamer growing. Deceleration of the electrons is accompanied with their diffusion during the time of displacement of ions toward the cathode (see Fig. 7), which will decrease a density of the electron layer and weaken the field between the electron layer and the anode. An increase in the distance between the charges will reduce a contribution of the radial component of the ion field that is closed on the electrons on the anode side (see Fig. 12). Eventually, the electron layer under exposure to the attracting force will begin its accelerated motion to the ionic layer, when its velocity vector of plasma oscillations will be directed toward the ions. An increment of the field energy obtained from the source will be spent for an energy supply of the electrons which ionize the gas.

Due to large values of the electric field strength in the double layer ($E_{d.l} \approx 5.4 \times 10^5$ V/cm) and a high coefficient of ionization in the CF_4 gas amounting to ≈4000–5000 cm^{-1} [46], it is sufficient for the electron layer to travel a single ionization length ($\alpha^{-1} \approx (2–2.3) \times 10^{-4}$ cm) in order to create a new pair of layers containing $(1–2) \times 10^8$ particles each. Fast electrons (approximately 30% [18]) of the new layer create, in turn, the next double layer, etc.

Since an ionization wave performs work by using the energy accumulated in the "capacitor" (double charge layer) when the ionic layer displaces to the cathode, then the power supply is not providing energy for ionization, and the drift current is absent. Additionally, the ionization wave resides between two ionic layers, which shield its motion from the chamber's anode and cathode. Therefore, there are no bias currents before and behind the ionization wave. The growth of a streamer branch will terminate when a distance between the last electron layer and the vanguard layer of ions becomes less than the ionization length. The last electron layer under exposure to repulsive forces from electron layers of the streamer branches will merge with the vanguard ionic layer. The created plasma system will collapse quickly without receiving energy supply.

The branch-by-branch growing of a streamer will be accompanied by light pulses caused by inflow of the current in each new branch. In experiments for optical observations of discharge, this effect was observed as a scintillating mode of the breakdown [24, 25].

From the energy viewpoint, the termination of streamer growth may be estimated as follows. The energy yielded by the power supply for a displacement of the ionic layer, containing 10^8 ions, by a value of the streamer-branch length (roughly equal to the oscillation amplitude [19] $\Delta x \approx 2 \times 10^{-2}$ cm) is defined by the expression

$$A = \frac{(e \cdot N_i)^2}{2 \cdot \epsilon_0 \pi R_0^2} \cdot \Delta x = 6.4 \times 10^{-8} \text{ J} \approx 4 \times 10^{11} \text{ eV}, \quad (6)$$

where $R_0 = 1.2 \times 10^{-2}$ cm is the radius of the electron "plate" or the streamer radius. On this length, 20 double layers are formed (see below). The energy required for creating a double layer is $\approx 3.2 \times 10^{-9}$ J. This energy is provided at the electric field strength of the "capacitor" $E \approx 10^4$ V/cm. Consequently, if the electric field created by charges of the double layer is lower than this value, then the streamer will not be able to grow.

Thus, a streamer ensures its advance owing to an increment of the electric field energy obtained from the power supply during the ionic "plate" displacement relative to the electron one, rather than to a strong field before the streamer head ("capacitor"). The energy stored in the "capacitor" will be spent on energy supply of the electrons, which ensure the gas ionization in the region of ionization wave propagation. We point out that this mechanism depends only upon a power supply capacity providing a sufficient current for the fast charging of "capacitors" of the ionized channel and is independent of the external field value.

In [11], it is noted that with lengthening of the ionized channel by a distance equal to a few radii of the streamer head, the field created by the channel charges near the head, as well as the radius of the head itself, is almost unchanged. This may be explained by the fact that the initial vanguard ionic layer after collapse is replaced with the last ionic layer of the first branch of the streamer. The new head of the streamer is again exposed to the cathode-directed driving force, and all processes forming the next branch of the streamer are repeated.

A fast formation of each branch of the streamer at the velocity $v_{str} = e\mu_e n_i R_0/2\epsilon_0 \approx 5 \times 10^8$ cm/s terminates in the channel stoppage for 1–1.5 ns, which is necessary for the passage of the ionic layer to the cathode to ensure the energy conditions for creating the next branch of the ionized channel. A structure of the ionized channel that is formed from the double charge layers is a steamer. *The presented process reflects a mechanism of growth of a streamer as an ionization wave, whose profile is equal to the thickness of electron layer* ($\approx 3 \times 10^{-4}$ cm)*, while a front width equals the lateral size of the formed ionized channel, i.e.,* $S = \pi R_0^2$ [22]. Let us note that the presented above mechanism of growing of the streamer channel is closest to the mechanism discussed in [11], which is based on propagation of the ionization wave with a very small transverse size comparable with a width of its front.

Figure 13 shows a photograph of the streamer burst which was obtained by means of the high-speed CCD camera PicoStar HR12 [47]. The photo perfectly confirms the stated above mechanism of growing a streamer as separate branches. The authors defined these branches to be a fine structure of the streamer. *According to our ideas, the streamer branches have a hyperfine structure in the form of double charge layers, owing to which the dynamic stability of the streamer and its energy supply are ensured.*

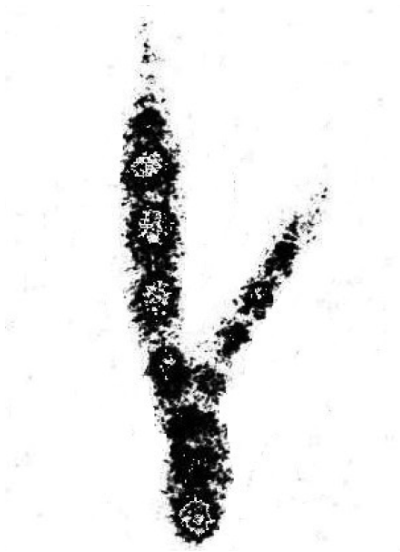

Fig. 13. Photograph of the cathode-directed streamer in the stroboscopic regime with $p = 740$ Torr, $U = 30$ kV.

In this system, owing to the long-range Coulomb interaction between the opposite charged layers, the energy transfer from the quasi-oscillating electrons to ions [10] must occur. A rate of energy transfer to ions from electrons in the streamer, when their temperature is higher than the ion temperature, according to [10], is defined by the formula

$$\frac{d\epsilon}{dt} = \frac{4\pi n_e Z^2 e^4}{m_i v_e} \cdot \ln\Lambda, \qquad (7)$$

where n_e is the electron density, v_e is the oscillating velocity of electrons, Z is the charge of CF_4. With $T_e = 3$ eV and $n_e = 3.5 \times 10^{14}$ cm^3, the Coulomb logarithm $\ln\Lambda = 7.47 + 1.5\log T_e$ [K] $- 0.5\log n_e \approx 8$. Hence, according to Eq. (7), *a rate of the energy transfer from electrons to ions will be* $d\epsilon/dt \approx 10^7$ eV/s. For transfer of the energy of the order of 0.5 eV to ions, the time 4×10^{-8} s will be required, which will allow elevating of the ion temperature to ≈ 5800°C and removing the capture of avalanche electrons by oxygen atoms.

A peculiarity connected with the system stability arises in the formed structure with the alternate charge layers. Let us consider three alternate layers located inside the ionized channel (see scheme 1 in Fig. 14). We denote q_1^+ a charge of the ionic layer closest to the anode, q_2^- will designate a charge of the electron layer, while q_3^+ will stand for a charge of the second ionic layer. Moreover, a charge of the electron layer that resides between the ionic layers is $0.7|q_1^+|$ and $q_1^+ = q_3^+$. This system is in the unstable equilibrium which takes

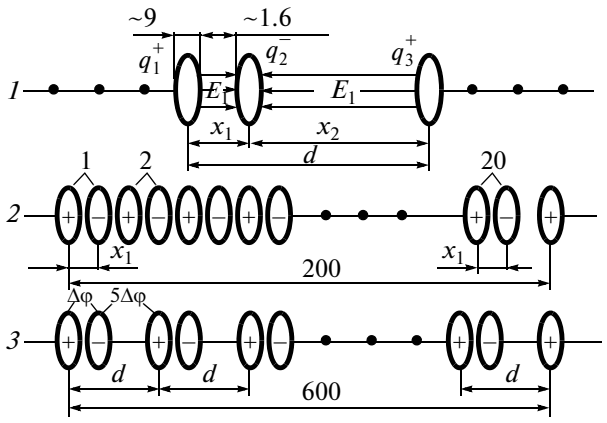

Fig. 14. Schematic structure of the ionized channel: (*1*) to calculation of the charge-system equilibrium; (*2*) the ionized channel after its completion; (*3*) the ionized channel after establishment of dynamic equilibrium. Distances are given in micrometers.

place when a sum of forces acting on each charge layer is equal to zero:

$$F_1 = F_2; \quad F_{13} = F_1; \quad F_2 = F_{13}, \tag{8}$$

where F_1 is the force of interaction between the charges q_1^+ and q_2^-; F_2 is the force of interaction between the charges q_2^- and q_3^+; F_{13} is the force of interaction between the charges q_1^+ and q_3^+. Let a distance between the charges q_1 and q_2 be x_1, a space between q_2 and q_3 be x_2, while a gap between q_1 and q_3 be d. Then

$$F_2 = F_{13} = \frac{1}{4\pi\epsilon_0}\frac{q_2^- q_3^+}{x_2^2} = \frac{1}{4\pi\epsilon_0}\frac{q_1^+ q_3^+}{d^2}; \quad \frac{q_2^-}{x_2^2} = \frac{q_1^+}{d^2}. \tag{9}$$

Since $|q_2^-| = 0.7q_1^+$, $x_2 = 0.836d$ and $x_1 = 0.164d$, where d is a distance between the ionic layers. The distance x_1 between the centers of gravity of the charges q_1^+ and q_2^- is set to be $\approx 5 \times 10^{-4}$ cm in the process of the avalanche evolution (a width of the electron layer is $\approx 3 \times 10^{-4}$ cm and the ionization length $\alpha^{-1} \approx 2 \times 10^{-4}$ cm, see below). Consequently, $d \approx 30 \times 10^{-4}$ cm, while $x_2 \approx 25 \times 10^{-4}$ cm. If the charge q_2^- approaches the charge q_1^+, then the attracting force between them will exceed the repulsive force from the charge q_3^+, and the equilibrium will be broken. The charges q_1^+ and q_2^- will merge with each other, while the charge q_3^+ will begin moving to the cathode. However, if there are alternate layers available on the left of the three-layer system (see scheme 2 in Fig. 14), then they will hinder the approach of the charges q_2^- and q_1^+ and enhance the repulsive action of the charge q_3^+. However, as soon as the charge q_3^+ will move a distance x_2 away from the electron layer, condition (8) begins to hold, and it will stop. In this case, a difference in potentials between the layers q_2^- and q_3^+ will increase up to $\Delta\varphi_2(x_2/x_1) \approx 5\Delta\varphi_2 \approx 360$ V and the field between the charges q_2^- and q_3^+ will become equal to the field between the charges q_1^+ and q_2^-. To fulfil the equilibrium condition (8) in the channel, it is necessary that the distances were settled to the values x_1 and x_2 (see scheme 1 in Fig. 14). If a distance of $2x_1 \approx 10 \times 10^{-4}$ cm between the similar charge layers in the growing channel is assumed to be a step of avalanches, then 20 double layers have to form on the displacement length of ionic layer equal to the amplitude of ion oscillations $a_i \approx 2 \times 10^{-2}$ cm (see scheme 2 in Fig. 14). The channel growing will be accompanied by establishment of the distances x_1 and x_2. Establishment of distances between the channel's layers will occur at a velocity equal to the velocity of ions; therefore this process is substantially slower than the process of channel growing. As a result, the channel length will increase up to $L_{ch} \approx 20d \approx 600$ μm (scheme 3 in Fig. 14).

The alternate double layers can be presented as *capacitors connected in series, across each of which the potential difference of* $\Delta\varphi_2 \approx 72$ V *or* $5\Delta\varphi_2 \approx 360$ V *is set in turn*. According to the estimations performed in [22], the potential difference across a length of the channel 600 μm long will be equal to $\Delta\Psi_{2k-1} = k\Delta\varphi_2 + (k-1) \cdot 5\Delta\varphi_2$, where k is the number of double layers. With $k = 20$, $\Delta\Psi \approx 8900$ V. *Owing to the potential difference, a portion of the current regularly flows into the ionized channel for charging of each new branch of the streamer formed during its growth*.

An issue of stability of alternate charge layers is the determining one; therefore, let us consider it in more detail. After the distances x_1 and x_2 have been settled, the distances between the channel's similar layers will be equal to the "dynamical constant" d (see schemes 1 and 3 in Fig. 14). The electric field inside each double layer will be equal to a sum of the fields created separately by the electron and ion charges. In the static state, the field in the domain where electron layers are located must be zero (see scheme 1 in Fig. 14). However, due to diffusion, collisions with molecules, and ionization inside the layer, its electric charge is subject to the permanent change in time. The radial displacement of electrons is very limited by the field of ions; therefore, all perturbations will occur, mainly, in the longitudinal direction between the layers.

Because perturbations arise in a fluctuating way, a time-varying electric field will appear in the channel. Owing to this field, a coupling is ensured between lay-

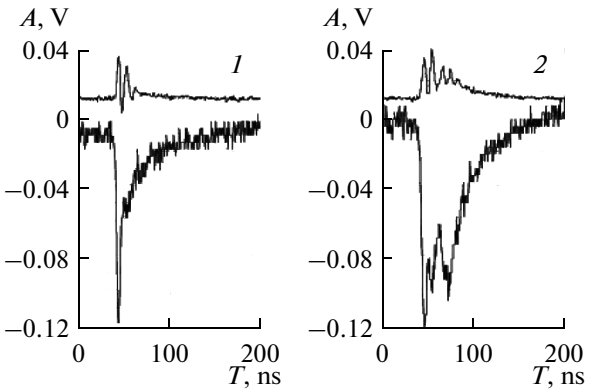

Fig. 15. Streamer formation in the gas mixture 90% CF_4 + 9.88% C_4H_{10} + 0.12% Hg. The attenuation of anode signals is 10 dB (lower oscillograms).

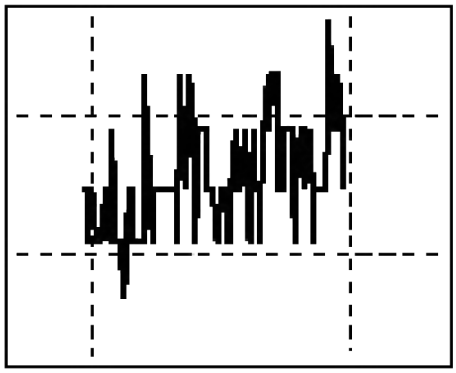

Fig. 16. Illustration of a behavior of electron layers in the ionized channel.

ers and any local changes arising in them are instantly transmitted along the channel length. Even the least deviation in the behavior of electron layer will induce a strong electric field preventing the further deviation. This property of the charge system, as well as the "constancy" of distances between ionic layers due to their inertia, cause the electron layers to be in the dynamical state within their equilibrium domain. Therefore, for sustaining the channel stability, electron layers under influence of the varying electric field will be in the quasi-oscillating motion with the varying period and amplitude. Figure 15 (especially its panel 1) shows that electrons are in the quasi-oscillating motion with the varying amplitude and frequency. The onset of transition from the plasma mode [18] to the streamer mode is the instant of emergence of high-frequency oscillations which have been superimposed on the trailing edge of a current signal on the anode during the chamber operation in the plasma mode. Figure 16 displays a fragment of the lower oscillogram from panel 1 in Fig. 15, which demonstrates a behavior of electron layers in the channel. The approximate structure of the stationary ionized channel may be presented as is shown in Fig. 14 (scheme 3). From the considered above structure of ionized channel and processes occurring inside the channel, it follows that *if, due to any external reasons, the streamer (or leader, see below) closes on itself, then the created neutral ionized channel will transit to a stable state with a long lifetime owing to the energy stored in the "capacitor".*

Summing up the experimental investigations of the electron avalanche evolution in wire chambers in the high gas-gain mode, the following may be stated: *for forming a double charge layer in the electron avalanche and for manifestation of the physical processes that provide the electron avalanche-to-streamer transition, the fulfilment of condition (2) is required, i.e., in the unit volume of the avalanche that is equal to* α^{-3} cm^3*, the number of electrons* N_e *must be* $\geq N_{cr}$*. For the avalanche-to-streamer transition, it is sufficient that the electric field* $E_{d.l}$ *created by charges inside the double layer, with the removed external field, be comparable with the resulting field* E_1^- *(immediately behind the electron layer) and less than the resulting field* E_1^+ *(behind the ionic layer)* [22].

The oscillograms showing the streamer formation are given in Fig. 15. Panel 1 in Fig. 15 illustrates a current signal from the ionic layer during its displacement toward the chamber cathode. The displacement of ions began with the fall of current signal corresponding to the plasma mode which can be easily identified by its very small duration. It can be clearly seen that the superimposed-signal duration, 150 ns, corresponds to the duration of the signals formed in the self-quenching streamer mode [20, 21] and is approximately 30 times larger than duration of the signal created in the plasma mode [18, 19]. In Fig. 15, panel 2, the formation of two streamer branches is shown. The upper oscillogram from the check wires displays the formation of two double layers, from which two streamer branches grow (clearly seen on the lower oscillogram).

Based on the experimental data set forth, we give a definition of streamer: *a streamer is the sequence of alternate electron and ionic layers, the dynamic stability of which is provided by the quasi-oscillating movements of electrons in the self-consistent electric field. Owing to the large storage of internal energy localized in double charge layers ("capacitors"), the energy supply of the streamer is implemented during its lifetime both in the external electric field and without it.*

Let us note that the information about new transient physical processes accompanying the electron avalanche-to-streamer transition is obtained in the narrow-gap multiwire chambers. As investigations have shown, they are a convenient instrument for studying a domain of avalanche-to-streamer transition owing to their high time resolution and capability of receiving information about the inductance value of

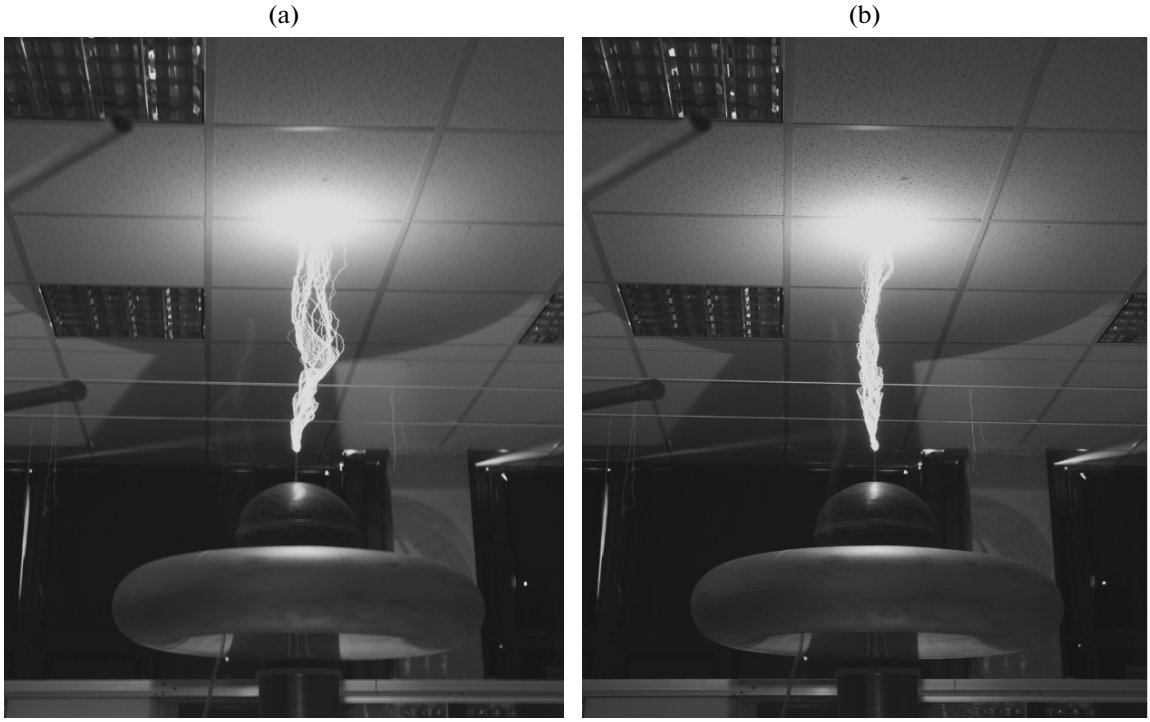

Fig. 17. Discharge of the Tesla transformer at excitation energy of (a) 25 J and (b) 27 J with the exposure time 0.1 s.

avalanche charges from several electrodes simultaneously. These properties of narrow-gap chambers distinguish them qualitatively from techniques used in the gas discharge physics.

Thus, studying and analyzing the described above processes revealing themselves in the prestreamer region of gas discharge allows the making of a conclusion that they are, in essence, the attendant processes that ensure the electron avalanche-to-streamer transition and may be interpreted as manifestation of properties of the double charge layer located in the external electric field. Dynamics of streamer formation displays stages of the consecutive transition of a streamer discharge to the qualitatively new, more complicated structurized states, where an increase of the internal consistence of charge systems occurs, due to which the stability of ionized channel is ensured.

The model based on new experimental data allows describing of all processes associated with growth and formation of the streamer both in a strong external field and in a weak one. From the model, a structure of the streamer and a cause of its stability follow; the mechanisms of emergence of seed electrons and an ionization wave, as well as the cause of fast heating of the ionized channel, are clarified. The model also makes it possible to elucidate mechanisms of proceeding of the phenomena that have been detected recently in lightning discharges, e.g., production of neutrons and coherent radiation.

Below it is shown how the pressing problems of a lightning discharge can be solved from the viewpoint of the presented model.

3.1. Avalanche-to-Streamer and Streamer-to-Leader Transitions

Dynamics of the streamer formation has been shown in section 3; therefore, we will now proceed to discussion of a streamer-to-leader transition. If each "long streamer" located inside the cone of the streamer zone of a leader is considered as an element of the current, then a total current of streamers will create a magnetic pressure. Because the streamers do not form a unified plasma medium, a total pressure created by each of them will cause pinching of streamers to the cone axis.

In photographs (Fig. 17) made at the JINR DLNP using the Tesla facility, almost identical filaments of many streamers can be seen, which is the confirmation that an electron avalanche transforms to a streamer only when the specific charge density is reached in it [9–11]. The identity of streamers allows the conclusion to be drawn that their wave properties are identical. *Therefore the convergence of streamers may lead either to formation of the dense channel consisting of streamers (a radial field of ions will probably hinder this merging) or to interference of the electromagnetic waves created by electron layers oscillating with close phases in the streamers. These waves will unite into the resulting high-intensity wave, which will lead to its nonlinear inter-*

action with charge layers of the streamers. Under to the impact of the formed wave, "long streamers" with close phases of oscillating electron layers will merge, creating the denser leader structure that is similar to streamers.

A streamer corona in the lightning discharge contains roughly 10^5 streamers [10]. According to the data given in [10, 48, 49], an electron avalanche transforms in air to a streamer when the number of ions in it $n_i \approx 10^9$. These values are reached owing to the presence of water vapors amounting to 1.65% in the thunderstorm atmosphere [31]. The water vapors play a role of the electronegative impurity and ensure the avalanche development at higher voltages. Here a density of the avalanche and hence of all charge layers of the streamer is $\approx 10^{14}$ cm^{-1}. Let us assume that all electron layers of streamers start to oscillate with the same phases as a result of their interaction with an intense wave. This will allow them to merge into the leader channel during their pinching to the discharge axis and will increase the number of ions in every layer up to $N_i \approx 10^5 n_i \approx 10^{14}$. A radius of leader channel of the lightning R_l is ≈3 cm [11, 49]. Using these values, we will estimate a value of double-layer capacitance C_0 and values of the potentials (φ_+, φ_-) in the immediate proximity from their surfaces. The estimation of a distance between the layers yields the value $\approx 3 \times 10^{-1}$ cm. Consequently, the capacitance of each double layer of the leader channel is roughly $C_0 \approx \epsilon_0 \pi R_0^2/d \approx 8.34 \times 10^{-12}$ F. The potential created by the ionic layer near its surface $\varphi_+ \approx eN_i/\pi^2\epsilon_0 R_l \approx 6 \times 10^6$ V. Since the number of electrons is 30% less, the potential, created by the electron layer of the leader, will be equal to $\varphi_- \approx -4.2 \times 10^6$ V. The energy stored in the double charge layer of the leader is defined by the expression $w = C(\varphi_+ - \varphi_-)^2/2$ and is ≈867 J. The energy inserted to the lightning channel with the length $L = 3$ km by a pulse of current will be equal to $W = wL/d \approx 8.67 \times 10^8$ J. Precisely this energy is spent for preserving the channel structure in time. The leader energy is permanently sustained by the current flowing into the leader from the channel base, owing to a great difference in potentials across the ends of the leader channel. From estimation of the energy input into the lightning channel, it follows that the leader channel, owing to its structure consisting of double charge layers ("capacitors"), provides itself with the larger linear capacitance than the capacitance per unit length of the casing, which is created around the ionized channel by positive charges of the died-out streamers [12].

Referring back to Fig. 17, we note that the magnetic pressure due to a low current in streamers cannot completely compensate for the resistance of viscous atmosphere, which leads to emergence of the resulting force that causes the streamers to move along a spiral line.

3.2. Gas Temperature in the Channel

Due to inertia of ionic layers, a distance between them is almost unchanged, while electron layers near their equilibrium are in the quasi-oscillating motion with the varying period and amplitude (see Fig. 16). Owing to these oscillations, the dynamic stability of the streamer channel is ensured. In this system, the energy transfer from the oscillating electrons to ions must occur due to the strong Coulomb interaction between the unlike layers [10, 45]. A rate of the energy transfer to ions from electrons in the streamer, when the electron temperature is much higher than the ion temperature, is defined by Eq. (7) and equals $d\epsilon/dt \times 10^7$ eV/s.

For transferring the energy of the order of 0.5 eV to ions, it will take the time of 5×10^{-8} s, which will make it possible to rapidly increase the ion temperature up to ≈5800°C, to destroy negative ions, to retard recombination, and to create conditions for the associative ionization: $N + O \rightarrow NO^+ + e$.

3.3. Conductivity and Heating of the Leader Channel

According to existing concepts [11], at the contact with the ground, the leader head of lightning acquires the ground potential and its charge almost instantly drains into the earth. This "relaxation" occurs by means of propagation of a wave of neutralization of the leader charge along the channel from the ground to the cloud (this wave is called the arrow-shaped leader). A velocity of the arrow-shaped leader approaches the speed of light and amounts to $(0.3–0.5) \times 10^8$ m/s. The motion is accompanied by a bright glow of the wave front. Between the wave front and the ground, a heavy current flows through the channel that carries away to the ground the charge from the "relaxing" sections of the channel. The amplitude of the current depends on the initial potential distribution along the channel. On average, it is close to 3 kA, while for the most powerful lightnings, it reaches 100–200 kA. The transport of such heavy current is accompanied by the intense energy release. Owing to this, the gas in the channel is heated rapidly and expands: a shock wave arises.

The lightning channel discharges at the velocity of arrow-shaped leader v_{ar} which is two to three orders of magnitude higher than a velocity of growth of the stepped leaders v_L. Accordingly, the channel's discharge current is $v_{arr}/v_L \approx 10^2–10^3$ times higher than the leader current $I_L \approx \tau_0 v_L \approx 100$ A. The channel's resistance per length R_0 should also reduce by roughly the same factor during the transition from the leader stage to the main one. The channel heating during the passage of heavy current is suggested to be the cause of reduction in the resistance [11].

However, the obvious contradiction follows from the statements above. Indeed, before the contact of the stepped leader with the ground, the channel had a high

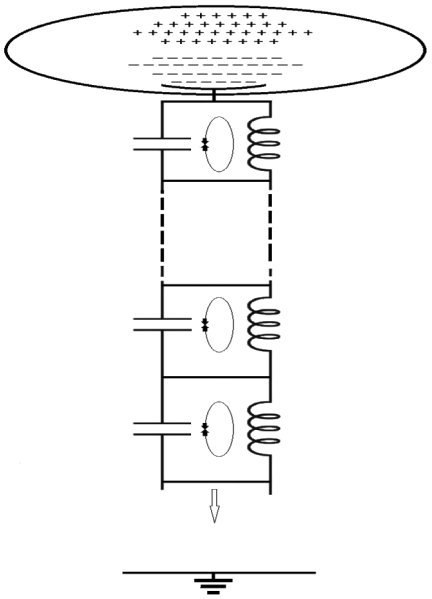

Fig. 18. Equivalent circuit of the structure of a leader that grows toward the ground. Arrows indicate the alternate change in the current direction in oscillating loops.

resistance capable of passing a current of no more than 100 A. The neutralization-wave propagation along the channel from the ground to the cloud at the velocity comparable with the speed of light ($\approx 0.5 \times 10^8$ m/s) does not mean that it is some electromagnetic perturbation. As a matter of fact, it is a phase velocity of the process [11]. However, as investigations indicate, a high velocity of propagation of the return wave of current is observed in the same channel. It is possible only in the case when the specific resistance of the channel behind the wave front of the lightning's main stage in the stationary state will be $R \approx 10^{-3}$–10^{-4} Ω/cm, while the total ohmic resistance of the entire lightning channel with a length of a few kilometers has to be of the order of 10^2 Ω [11]. In other words, we have mutually exclusive requirements: in order to heat the channel for the purpose of reducing its resistance, a large current is needed, but in order to obtain a large current, it is necessary to heat the channel. From here it follows that just as the leader current flowed in the channel, so it will flow in the stepped leader, inducing no sharp changes. **Consequently, a high temperature of the ionized channel has to be ensured by the certain process occurring simultaneously with the stepped-leader channel of the lightning growing toward the ground.**

According to the stated above, a leader by its structure is a system of double charge layers—"capacitors" connected in series—which may be called "energy-storage capacitors". At each step of the leader growth, the current inflow from the thundercloud to the "energy-storage capacitors" provides them with energy. A part of this energy goes to sustaining the oscillating electron layers, i.e., the channel structure. Since the only limitation for a current of the leader during its growth is its conductivity, the "energy-storage capacitors" with a gap between the "plates" amounting to $\approx 3 \times 10^{-1}$ cm are charged up to breakdown. Therefore the ionized channel of lightning is always in the **discharge mode** until the completion of the lightning's main stage. This mode of operation is implemented due to high power of the thundercloud (100–1000 MW [3]). We note that namely the breakdown of "energy-storage capacitors" is the main source of glowing of steps of the leader channel during the current inflow into them. In the case of multicomponent lightning, all processes are repeated. During the breakdown, streamers are created that close the "plates" of the "energy-storage capacitors," which are distributed over the cylindrical surface along the channel of the stepped leader. The closed streamers with the inductivity $L = nL_0 = n(\mu_0/2\pi)\ln(d/r_0) = n \cdot 2 \times 10^{-7}$ H/m (L_0 is the inductivity of a single closed streamer, $r_0 = 10^{-1}$ cm is the radius of the closed streamer, n is the number of closed streamers), together with the "capacitors," create parallel oscillating loops. A sequence of these oscillating loops forms the ionized channel of the descending leader (Fig. 18). An arc drawn above the inductive-capacitive system (see Fig. 18) reflects the "capacitive" coupling of the channel with the thundercloud charges.

The energy, spent by "capacitors" during their breakdown for heating of the downward leader and conservation of its structure, will be constantly replenished with the thundercloud current, which is the leader current I_l over the period of the leader growing toward the ground. Let us note that while the leader is not earthed, the energy exchange between the inductance and the "capacitor" will occur permanently in parallel loops. The duration of every such cycle is equal to $t = \pi \cdot \sqrt{CL} = 5.7 \times 10^{-9}$ s. Owing to the current closure in each oscillating loop (see Fig. 18), the energy in them is accumulated by turns: either in the form of the electric field energy of the charged capacitor, or in the form of the magnetic field energy of the inductance. In this case, the natural loop current $I_{l.c}$ flows in the oscillating loops, which is Q times higher than the supply current of the growing leader $I_l \approx 100$ A (Q is the Q-factor of the oscillating loop). Thus, during the time of leader growing toward the ground, a heavy closed current circulates in each oscillating loop that produces the permanent heating of the corresponding sector of closed streamers. The leader earthing will lead to the uniform distribution of the existing difference in potentials of opposite sign between the ground and the cloud on the similar double charge layers—"capacitors". The ionized channel of the negative downward leader will not simply lose its negative charge in this case but also will acquire the positive charge, i.e., it is not only discharged but also recharged. When the "capacitors" are recharged, their energy does not drop down to zero since a new differ-

ence in potentials is set on them which is determined by the "cloud–earth" voltage.

The distribution of the new potential difference (or the neutralization wave [@30]) occurs at a velocity of $\approx(0.3–0.5) \times 10^{10}$ cm/s. In this case, the "capacitors," in accordance with this velocity, are discharged onto the heated closed streamers, and **the heavy current instantly drains into earth via them** (Fig. 19).

The recharging of capacitors at the moment when the "earth–cloud" potential is distributed over them is accompanied by their discharge, which is the cause of glowing of the wave front—arrow-shaped leader. *Since the discharge current of "capacitors" is localized in plasma filaments residing on the cylindrical surface beyond the leader channel, effects related to heavy currents (heating and a shock wave) do not touch upon the leader channel and it remains intact for subsequent components of the lightning discharge*. A powerful pulse of the current flowing along the channel will also lead to phasing of electrons of the plasma filament and the electron layers, which additionally will reduce the channel resistance and allow passing of pulses of the current with the amplitude up to 200 kA. The return arrow-shaped leader travelling from the cloud to the ground at the velocity of $\approx 10^7$ m/s [11] will rapidly charge the discharged "capacitors" of the leader channel. A contact of the current with the ground again will lead to polarity reversal of potentials on double layers and to their subsequent discharge. For multi-component lightnings, the processes described above recur repeatedly. We note that owing to the proposed structure and heating mechanism of the leader channel, the energy loss for heating of the ambient cold air reduces to a minimum.

Specific features of charging and discharge of "energy-storage capacitors" whose "plates" consist of electron and ionic layers should be also stressed. Since a charge of layers is unchanged, charging of the "capacitor" is expressed in increasing distance between the "plates," due to which the potential difference grows on them; hence, the "capacitor" energy also increases. A discharge of these "capacitors" (with recharging to smaller potentials) is accompanied by reduction in the gap between the layers.

As regards lightning, the charging of "energy-storage capacitors" is accompanied by an increase in the effective length of the lightning and the speed of its growing toward the ground. The recharging of the "capacitors" and their subsequent discharge lead to a decrease in the length of the lightning, due to which its contact with the ground is broken. This, in turn, will make it possible to maximally charge the capacitive system of ionized channel and to heat the channel for the next lightning component.

The discussed mechanism of forming a high conductivity of leader channel allows one to consider an alternative interpretation of the mechanism of spark breakdown. **A pulse discharge of energy-storage capacitors forming the structure of a streamer or a leader, rather than a voltage supply, is the source of heavy current during a spark discharge.** In confirmation of the above, the streamer discharges obtained at the Tesla transformer of the JINR DLNP can be given. If a discharge propagates in air in the direction of the grounded conducting plane with an area of 110×110 cm but does not reach it, then the streamer channels have a weak luminosity and the total current created by them in the shunt at the earth end does not exceed 5 mA. If the streamers come into contact with the earthed plane, then they flare up brightly and a pulse current of 300–350 A passes through the shunt installed at the point of grounding of the conducting plane. It is evident that the Tesla transformer with a power of 5 kW and an output voltage of $\approx 10^6$ V cannot be a source of such heavy currents.

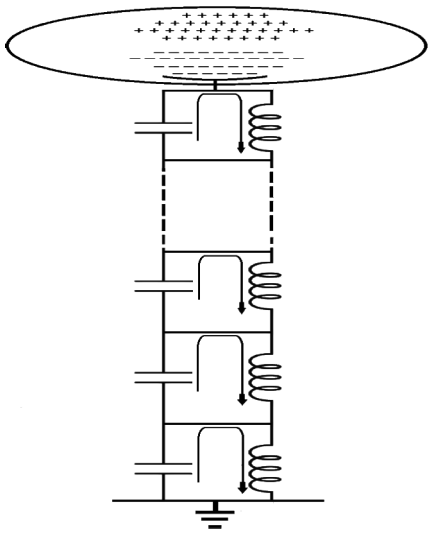

Fig. 19. Discharge of energy-storage capacitors at the contact of a leader with the ground.

3.4. Streamer Growth in a Weak Field

A potential of the vanguard ionic layer of the streamer (streamer head) in the lightning discharge near its surface is roughly $\varphi_+ = \sigma_+ R_0/\pi\epsilon_0 = eN_i/\pi^2\epsilon_0 R_0 \approx 1.8 \times 10^4$ V, where $R_0 \approx 10^{-1}$ cm is the streamer radius, and $N_i \approx 10^9$ is the number of ions [10]. This potential, together with the distributed potential from a source of external field, is needed above all for creating a potential jump on the positive surface of the streamer head (see Fig. 6) in order for the ionic layer under exposure to the emerged driving force (3) to begin its motion toward the cathode. Let us note that the similar mechanism of the potential jump in the streamer head must be implemented in the flat spark gap due, to which the electric field in the region of streamer growth becomes inhomogeneous.

A potential of electron layer in the streamer head will be $\varphi_- = 0.7\sigma_+ R_0/\pi\epsilon_0 = -eN_i/\pi^2\epsilon_0 R_0 \approx 1.2 \times 10^4$ V.

Consequently, a potential difference between layers will be $\Delta\varphi \approx 3 \times 10^4$ V. An electric field strength and a distance between the electron and ionic layers are $E = \sigma/\epsilon_0 = 5.75 \times 10^4$ V/cm and $h = \Delta\varphi/E = 0.52$ cm, respectively. According to [51], the effective coefficient of ionization $\alpha_{\text{eff}} = (\alpha - a)$, where a is the coefficient of adhesion of electrons to oxygen, with $E/p = 75.65$ V/(cm Torr) is 90 cm^{-1} [12].

With this coefficient of ionization, the seed electrons (in number of $N_0 = 3 \times 10^8$) will create as a result of breeding the next double charge layer with the number of ions $N_i = 10^9$ on the length x. We will find the ionization length x from the expression for the gas gain—multiplication factor $M = N_i/N_0 = \exp(\alpha x)$, i.e., $x = \ln(N/N_0)/\alpha = 0.0366$ cm. Consequently, a single branch of the growing streamer in the lightning discharge will contain $h/x \approx 14$ double charge layers.

A work that the power supply or the thundercloud performs against electrical forces while ions travel a distance h is completely consumed for increment of the "capacitor" field energy. The work value is defined by Eq. (7) and equals $A = \Delta W = 2.4 \times 10^{-6}$ J $= 1.5 \times 10^{13}$ eV. The energy in the double charge layer received from the power supply will be spent on the energy supply of electrons. They will produce the gas ionization inside the "capacitor" during their motion to the vanguard ionic layer. The stored energy is quite sufficient for creating 14 double charge layers in the process of ionization.

Thus, propagation of the ionization wave (streamer growing) depends only upon the power supply capacity, which provides the sufficient current for the rapid charging of "energy-storage capacitors" of the ionized channel and is independent of the external field. A strong external field (≥30 kV/cm) *has to be present in the thundercloud only in the region of development the very first electron avalanches which are the beginning of the lightning discharge formation.*

3.5. Generation of Coherent Super-High-Frequency Radiation of a Leader

As has been shown in [51–53], the intense coherent radiation may arise in the electron bunches when their sizes are less than a wavelength of the radiation itself. A radiation power must be proportional to a square of the number of particles in the bunch. The induced radiation in these spatially-localized excited ensembles with a large lifetime of electrons arises as a result of their self-organization when phasing of electrons occurs with the subsequent coherent release of the stored energy (as light). This phenomenon is called superradiance.

As has been noted above, the streamer and leader structures completely satisfy the conditions of emergence of the coherent radiation: electrons and ions of the streamer channel are grouped into the narrow layers ≈3×10^{-4} cm thick with a density of 10^{14} cm^{-3} [22]; a thickness of the leader layer with the same density is ≈180×10^{-4} cm. For ensuring the dynamic stability of the ionized channel, electron layers must be in the quasi-oscillating state. Closing of the external potential difference by the ionized channel will lead to the uniform distribution of potentials on the identical double layers ("capacitors") and will recharge the capacitive system of the ionized channel. In the process of recharging of "energy-storage capacitors", their discharge will happen. A current of the leader channel will rise abruptly up to a few tens of kiloamperes, which will ensure a powerful energy inflow to the lightning channel. Owing to a pulse of the very heavy current, the electrons will transfer from the quasi-oscillating movement to the ordered oscillating motion with the same amplitude, i.e., phasing of oscillations of electron layers will occur along the entire channel length. The emerged system will try to maintain the stable state; therefore, any energy excess in the channel will be emitted into the environment. As a result, a part of energy of the ordered motion of electrons will transfer to the energy of the coherent electromagnetic radiation.

3.6. Neutron Production in a Lightning Discharge

To deny the possibility of proceeding of a fusion reaction in lightning discharges is the main fallacy, since in the structure of the lightning channel, there is a mechanism of energy transfer from the oscillating electron layers to ions. According to experimental data, the production of neutrons occurs at the instant of development of the main return shock, which is accompanied by a return wave of the current with the amplitude of up to 200 kA. This current provides the energy for the inductive-capacitive system distributed in the channel. The stored energy in the storage elements can be transferred to ions in the process of oscillations. This mechanism owing to the high frequency and rate of the energy transfer allows a fusion reaction to be triggered at lower energy in a lightning discharge. This is an advantageous distinction of this mechanism of fusion reaction from the one used in tokamaks.

It has been shown above that owing to long-range action of Coulomb forces, a fast heating of the ionized channel occurs to the temperatures at which a capture of electrons by oxygen comes to an end. However, in phasing of electrons, during the return shock, it is easier to use a more efficient mechanism of energy transfer from the oscillating electron layers to the ionic layers. According to the theory of oscillations, in the system consisting of two elastically coupled pendula, the time of half-energy transfer from an oscillating pendulum to an immobile pendulum is defined by the expression [45]

$$t = \frac{\pi}{\omega\gamma_2}, \tag{10}$$

where for our case, ω is the oscillation frequency of electron layers; γ_2 is the value of the elastic coupling forces between electron and ionic layers (see Eq. (4)). According to measurements performed in [27, 28], a radiation frequency during the main stage of lightning (return shock) is 30 GHz with a total duration of coherent radiation of electrons amounting to 60 μs. A return shock is accompanied by a powerful current pulse with the amplitude of up to 100–200 kA, which will ensure the phasing of electrons and increase their oscillation amplitudes in the vicinity of points of static equilibrium. The increase in the oscillation amplitude of electrons will lead to the growth in forces of binding γ_2 in Eqs. (10) and (4), which will decrease the time of energy transfer to ions. According to [10, 49], the temperature of ionized channel during the return shock reaches ≈20000–30000°C (≈1.7–2.6 eV). A value of the coefficient γ_2 is roughly 10^{-2}, and the transfer of 1 eV to ions, according to Eq. (10), takes the time of the order of 1.6×10^{-10} s. For the time of exposure to the main shock equal to 60 μs [27, 28], the energy of electrons will be sustained by a powerful current pulse, and the electrons can transfer approximately 4×10^5 eV to ions over this period of time. This pumping results in the intense electromagnetic radiation of the lightning within a broad wavelength range from fractions of micrometer to a few meters (it is not connected with bremsstrahlung of fast electrons) [4].

According to [32], a relative water vapor concentration in the gas atmosphere is 1.65%, while a concentration of deuterium molecules in the natural water is 0.015%. Consequently, the number of deuterium ions contained in each ionic layer of the lightning channel will be $\approx 2.5 \times 10^8$. The deuterium ions reside in the leader's ionic layers and are located between the oscillating electron layers, which are coupled with ions by means of strong electric fields. With phasing of oscillations of the electron layers during the return shock, the electrons with a frequency of 30 GHz [27] will transfer the energy of up to 400 keV to the ions. If 1000 pairs out of 250 million deuterium ions find themselves in the immediate proximity to each other, then they with a great probability will be able to overcome the electric repulsion and to approach each other within a distance of action of nuclear forces, i.e., enter the reaction of fusion. With the number of double charge layers amounting to $\approx 10^6$ and the lightning length to be 3 km, the number of neutrons will be $\approx 10^9$, which agrees well with the result obtained in [29].

3.7. Lightning Protection

Photographs given in Fig. 1 demonstrate how the Eiffel and Ostankinskaya Towers were found to be unprotected. The situation can be explained, strangely enough, by the presence of pointed spires at them. Lightning, as has been shown in section 3.3, represents the energy system of "energy-storage capacitors", in which the electric field energy is concentrated (see section 3.3). The energy is supplied from the thundercloud, the electric power of which is 100–1000 MW. Let us note that a part of this energy goes to the growth and sustaining of the leader channel. It is shown in section 3 that in the front of the growing ionized channel, there is a layer of positive ions that creates in its vicinity the potential of the order of $eN_i/\pi^2\epsilon_0 R_l \approx 6 \times 10^6$ V. On the lightning-protection rod, a positive charge is also induced, a value of which depends on the rod height. The lightning transfers the energy, stored in capacitors, to the lightning-protection rod. However the rod, separated by the earthing-bus inductance and the ground-loop impedance from the ground capacitance, is often unable to receive and transmit the lightning energy.

Assuming the described above structure of leader channel consisting of a sequence of "energy-storage capacitors" in which the energy is concentrated, the simplest way for lightning to release the stored energy is to give it to another capacitor. Since the "energy-storage capacitors" of the ionized channel are connected in series, then their total capacitance is very small. Therefore, if the rod is replaced with the special design capacitor of roughly 100–200 pF, then the lightning, created in the zone of the lightning-protection coverage, must "see" it because the discharge propagates in the direction of the larger capacitance and higher conductivity. In capacitive systems, a current leads a voltage by $\pi/2$ in phase; therefore, while the capacitor is not charged, the distributed parameters of earthing do not influence the capture of the lightning by the lightning-protection.

In order to answer the question of whether this lightning-protection system is suitable for large-scale application, detailed studies are necessary. Moreover, no other methods for increasing the efficiency of action of lightning-conductors are offered now.

3.8. Ball Lightning

Ball lightning, as a rule, is observed during a thunderstorm and its appearance is related to linear lightning-discharges. A problem in comprehension of the ball-lightning nature is determined, to a greater degree, by lack of sufficient information concerning properties of linear discharges.

It is known that numerous observations of ball-lightning behavior made it possible to refine the questions which the proposed model of physical nature of ball lightning must answer, e.g., the questions taken from Internet:

1. Why is ball lightning a very rare phenomenon?

2. Why is ball lightning so stable?

3. After all, if it is a gaseous formation, then this gas or plasma immediately will shuffle with the ambient air. What hinders this mixing?

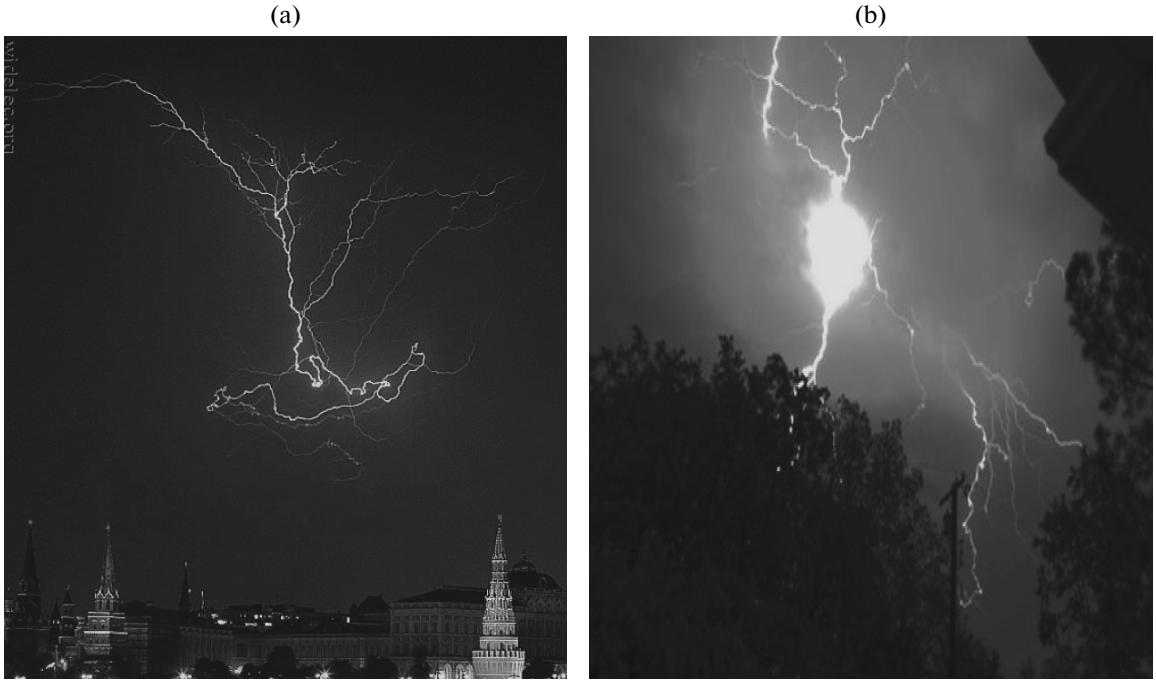

Fig. 20. (a) Unpredictability of the lightning path. (b) Origination of ball lightning.

4. Where does this stability of shape come from? This must mean the presence of the fairly strong surface tension on the border separating ball lightning from the surrounding atmosphere. Why is it possible at the interface of two gases?

5. Why does ball lightning not rise? After all, a hot gas cloud should float up when exposed to the force of Archimedes.

6. How can ball lightning exist over such a long period of time? After all, if there is plasma inside it and if there is no energy supply from outside, then why does the plasma not recombine instantly? Maybe, there is some external energy feeding that is sightless with human eye?

7. From where do these energy reserves in ball lightning come (after all, according to assessments, a typical ball lightning contains tens and hundreds of kilojoules)?

8. How can ball lightning go round an obstacle and flow through small holes? After all, if it is simply a charge, then it must be attracted to the surrounding bodies. Why do simple laws of electrostatics not manifest themselves here?

9. What is the reason for a strong electromagnetic radiation in the extraordinarily wide wavelength range from some fractions of millimeter to a few meters?

10. Why does ball lightning not radiate heat?

11. How is the ability of splitting-up of ball-lightning implemented?

12. Due to what processes can ball lightning explode spontaneously or while touching a subject?

13. Why are mostly metallic parts of subjects damaged and burned out during explosions (while dielectric parts remain intact)?

14. How does ball lightning pass through glass by burning a hole in it?

A photograph in Fig. 20a demonstrates a path of lightning motion. The lightning behavior is really unpredictable. The lightning orientation mainly depends upon the direction of the external electric field and the field of vanguard layer of positive ions.

It is known that at a height of ≥500 m, the different-density clusters create from the water vapor with dust impurity, on which the positive charge from the thundercloud is induced. The presence of these formations on the path of the growing discharge, in the front of which is a layer of positive ions, may have a substantial effect on its direction. This is clearly seen on the presented photograph. If a direction of resulting field makes the zigzag lightning close on itself (which may occur extremely seldomly), then the closed loop will become neutral and tear away from the main channel. While exposed to atmospheric pressure, the loop, being warmer than the ambient air and having therefore the smaller pressure, will take a shape of a ball, which we call "*ball lightning*" (Fig. 20b). Rolled into a ball, a part of the linear lightning maintains its structure, i.e., consists of the same double charge layers. Its dynamic stability is ensured by oscillating motion of electron layers. A large lifetime of the ball lightning is maintained owing to the significant store of energy concentrated in double layers (capacitors) and to the absence of the conduction current, i.e., there is no

Joule heat loss of the stored energy. For example, if a length of the separated part of a linear lightning is $l =$ 50 m, then the energy of the order of $W_{50} = wl/d = 10^7$ J will be concentrated in the ball. Relying on the structure and properties of a linear lightning, it is easy to continue the explanation of ball-lightning properties, but due to the limited scope of the article, we note that the proposed model of ball lightning is the only model which gives the simple explanation not only for the ball lightning origin but also for almost every property which it manifests in a free state.

4. CONCLUSIONS

We will give some conclusions that play, in our opinion, a great role in spark discharge, including lightning.

Based on experimental data obtained while studying in detail a domain of avalanche-to-streamer transition, a model of the structure of a streamer is developed with which the characteristic phenomena accompanying a lightning discharge are well agreed. A general picture of development of an ionized channel is described, and a model of the structure of a leader is presented which, as well as a streamer, consists of alternate double charge layers: electron and ionic layers. It is shown how the dynamic stability of ionized channel is provided. It is possible owing to the fact that electron layers execute quasi-oscillations in the self-consistent electric field that opposes to any changes in the ionized channel.

As compared with the model of plasma streamer, the proposed model [24, 25] with alternate charge layers is a more stable system, in which a plasma formation has transformed and changed to a new, more stable state with a large store of interval energy, and from which the external electric field is excluded.

The discussed process of heating the gas of the ionization channel owing to oscillations of electron layers allows the gas temperature to be elevated up to 5000–6000°C during $\approx 5 \times 10^{-8}$ s. Eventually, negative ions collapse, recombination decelerates, and the opportunity appears to implement the mechanism of associative ionization ($N + O \rightarrow NO^+ + e$).

It is shown that the mechanism responsible for propagation of the ionization wave, whose profile is equal to a thickness of the electron layer (while a width of front is equal to a transverse size of the created ionized channel), does not depend on the external field magnitude and is completely determined by the energy stored in the initial double layer that plays a role of "energy-storage capacitor." Electrons, residing in the front of electron layer and amounting to 30% their total number in the avalanche, serve as the seed electrons appearing before the front of ionization wave.

The proposed mechanism of transformation of a leader channel to a sequence of parallel oscillatory loops makes it possible to explain the heating of the ionized channel, the reduction in its impedance, and thus the creation of conditions for implementation of processes occurring in the main stage of lightning.

It is obvious that all observed processes revealing themselves at different stages of development of a lightning discharge cannot be taken into account in a single work. However, if the given above models of the structure of a streamer and a leader are taken as a basis, then the opportunity appears to answer the questions of how the majority of them proceed. For example, why the ionized channel does not emit light between the pulses, or why in the subsequent components of lightning, a reduction in their radii is observed.

Additionally, the proposed model of the structure of a leader channel (considered as an inductive–capacitive system) makes it possible, on the basis of its parameters, to determine the duration of implementation of processes and the time of transition between the processes and to derive equations of a long line with distributed parameters, which will make it possible (i) to analyze in detail the processes occurring in the line, (ii) to determine their main parameters at different points of the leader, and (iii) eventually to obtain a clear picture of dynamics of transformation of the leader channel for the main stage of lightning.

The experimental data presented in the work such as the photograph of streamer burst showing a nature of streamer growth (see Fig. 13), a tendency of streamers to merge (see Fig. 17), a value of discharge current at the Tesla transformer (see section 3.3), as well as the explanation of mechanisms of coherent radiation and neutron production in a lightning discharge, are in a full agreement with the stated ideas on the mechanism of spark breakdown and undoubtedly indicate that the chosen field of research is promising.

ACKNOWLEDGMENTS

The author is grateful to Corresponding Member of the Russian Academy of Sciences I.N. Meshkov for approval and encouragement of the work and for valuable suggestions that were taken into account in preparation of the manuscript for printing, to Prof. A.F. Pisarev for moral support and permanent attention to this work, to Prof. E.M. Syresin and to Senior Researcher L.G. Tkachev for careful reading of the manuscript and critical constructive suggestions.

The author thanks Prof. O.A. Zaimidoroga and Senior Researcher V.N. Pavlov for helpful discussions, owing to which many statements of the work were refined.

REFERENCES

1. *Problems of Atmospheric Electricity* (Gidrometeoizdat, Leningrad, 1969) [in Russian].
2. M. B. Baker and J. G. Dash, "Mechanism of charge transfer between colliding ice particles in thunderstorms," J. Geophys. Res. **99**, 10621–10626 (1994).

3. V. I. Ermakov and Yu. I. Stozhkov, Preprint No. 2 FIAN (Lebedev Physical Institute, Russian Academy of Sciences, Moscow, 2004).
4. A. V. Gurevich and K. P. Zybin, "Runaway breakdown and electric discharges in thunderstorms," Phys.-Usp. **44** (11), 1119–1140 (2001).
5. J. M. Meek and J. D. Craggs, *Electrical Breakdown of Gases* (Clarendon Press, Oxford, 1953).
6. L. B. Loeb, *Fundamental Processes of Electrical Discharge in Gases* (John Wiley and Sons, New York, 1939).
7. J. M. Meek and J. D. Craggs, *Electrical Breakdown of Gases* (Clarendon Press, Oxford, 1953; Inostrannaya Literatura, Moscow, 1960) [in Russian].
8. H. Raether, *Electron Avalanches and Breakdown in Gases* (Butterworths, London, Washington, 1964).
9. E. D. Lozanskii and O. B. Firsov, *Theory of the Spark* (Atomizdat, Moscow, 1964) [in Russian].
10. Yu. P. Raizer, *Gas Discharge Physics* (Springer, Berlin, 1991).
11. E. M. Bazelyan and Yu. P. Raizer, *Spark Discharge* (CRC Press, Boca Raton, 1998).
12. E. M. Bazelyan and Yu. P. Raizer, *Lightning Physics and Lightning Protection* (IOP Publishing, Bristol, Philadelphia, 2000).
13. A. F. D'yakov, Yu. K. Bobrov, A. V. Sorokin, and Yu. V. Yurgelenas, *Fundamentals of Electrical Breakdown in Gases* (Mosk. Energ. Inst., Moscow, 1999) [in Russian].
14. J. R. Dwyer and V. A. Uman "The physics of lightning," Phys. Rep. **534**, 147–241 (2014).
15. K. K. Darrow, *Electrical Phenomena in Gases* (Williams and Wilkins Co., Baltimore, 1932).
16. H. Kalmar, A. G. Ketikjan, E. V. Komissarov, V. S. Kurbatov, V. Z. Serdiuk, V. V. Sidorkin, A. V. Voskanjan, and B. Zh. Zalikhanov, "New method for constructing multiwire chambers," Nucl. Instrum. Meth. A **307**, 279 (1991).
17. H. Kalmar, A. Zh. Ketikjan, E. V. Komissarov, V. S. Kurbatov, V. Z. Serdiuk, V. V. Sidorkin, A. D. Volkov, A. V. Voskanjan, and B. Zh. Zalikhanov, "Development of the method of multiwire detectors working in high rate environment," in *Proc. of the 3rd Workshop on Physics at UNK* (Protvino, Russia, 1990), p. 31.
18. B. Zh. Zalikhanov, "Plasma mechanism of a discharge in wire chambers in high gas multiplication mode," Fiz. Elem. Chastits At. Yadra **29** (5), 1194–1258 (1998).
19. B. Zh. Zalikhanov, "Specific features of electron avalanche in high gas multiplication mode," Phys. Part. Nucl. Lett. **3** (2), 118–130 (2006).
20. G. D. Alekseev, V. V. Kruglov, and D. M. Khazins, "Self-quenching streamer discharge in a wire chamber," Phys. Part. Nucl. **13**, 293 (1982).
21. M. Atac, A. V. Tollestrup, and D. Potter, "Self-quenching streamers," Fermilab Report No. FN-348, 1981.
22. B. Zh. Zalikhanov, "Double charge layer in high-current electron avalanche," Phys. Part. Nucl. Lett. **3** (3), 211–221 (2006).
23. Yu. D. Korolev, and G. A. Mesyats, *Physics of Pulsed Breakdown in Gases* (URO Press, Ekaterinburg, 1998).
24. O. A. Omarov, *Pulsed Discharges in High-Pressure Gases* (Yupiter, Makhachkala, 2001) [in Russian].
25. O. A. Omarov and A. A. Rukhadze, "On the plasma mechanism of developing the early stages of breakdown in gases," Tech. Phys. **56** (7), 944–949 (2011).
26. T. H. Teich, "Emission Gasionisierender Strahlung aus Elektronen Lawinen," Z. Phys. **199** (4), 378 (1967).
27. V. F. Fedorov, Yu. A. Frolov, and P. O. Shishkov, "Millimeter electromagnetic radiation of a lightning return stroke," Prikl. Mekh. Tekh. Fiz. **42** (3), 9–14 (2001).
28. Yu. P. Vagin, K. S. Mozgov, T. A. Semenova, and V. F. Fedorov, "Coherent microwave radiation generated by strong atmospheric sources," Elektromagn. Volny Elektron. Sistemy, No. 3, 81–87 (2011).
29. A. V. Gurevich, V. P. Antonova, A. P. Chubenko, A. N. Karashtin, G. G. Mitko, M. O. Ptitsyn, V. A. Ryabov, A. L. Shepetov, Yu. V. Shlyugaev, L. I. Vildanova, and K. P. Zybin, "Strong flux of low-energy neutrons produced by thunderstorms," Phys. Rev. Lett. **108**, 125001 (2012).
30. B. M. Kuzhevskii, "Neutron production in lightnings," Vestn. Mosk, Univ., Ser. 3: Fiz. Astron., No. 5, 14–16 (2004) [In Russian].
31. L. P. Babich, "Generation of neutrons in giant upward atmospheric discharges," JETP Lett. **84** (6), 285–288 (2006).
32. B. E. Carlson, N. G. Lehtinen, and U. S. Inan, "Neutron production in terrestrial gamma ray flashes," J. Geophys. Res. **115** A00E19 (2010). doi:10.1029/2009JA014696
33. L. P. Babich, E. I. Bochkov, I. M. Kutsik, and A. N. Zalyalov, "On amplifications of photonuclear neutron flux in thunderstorm atmosphere and possibility of detecting them," JETP Lett. **97** (6), 291–296 (2013).
34. http://www.en.wikipedia.org/wiki/Ball_lightning
35. A. von Engel, *Ionized Gases*, 2nd ed. (Oxford Univ. Press, Oxford, U.K., 1965).
36. D. F. Frank-Kamenetskii, *Plasma—the Fourth State of Matter* (Plenum Press, New York, 1972).
37. R. Henderson, W. Faszer, R. Openshaw, G. Sheffer, M. Salomon, S. Dew, J. Marans, and P. Wilson, "A high rate proportional chamber," IEEE Trans. Nucl. Sci. **NS–34** (1), 528 (1987).
38. E. M. Gushchin, E. V. Komissarov, Yu. V. Musienko, A. A. Poblaguev, V. Z. Serdyuk, and B. Zh. Zalikhanov, "Fast beam chambers of the set-up ISTRA-M," Nucl. Instrum. Meth. A **351** (2–3), 345–348 (1994).
39. Yu. V. Zanevskii, *Wire Detectors of Elementary Particles* (Atomizdat, Moscow, 1978) [in Russian].
40. *Berkeley Physics Course,* Vol. 2: E. M. Purcell, *Electricity and Magnetism* (McGraw-Hill, New York, 1965).
41. J. Fischer, A. Hrisoho, V. Radeka, and P. Rehak, "Proportional chambers for very high counting rates based on gas mixtures of CF_4 with hydrocarbons," Nucl. Instrum. Meth. A **238**, 249 (1985).
42. B. Zh. Zalikhanov, Preprint No. OIYaI R13-2006-118 (Joint Institute for Nuclear Research, Dubna, 2006).

43. S. Majewski, G. Charpak, A. Breskin, and G. Mikenberg, "A thin multiwire chamber operating in the high multiplication mode," Nucl. Instrum. Meth. **217**, 265 (1983).
44. V. I. Bychkov, Candidate's Dissertation in Mathematics and Physics (Joint Institute for Nuclear Research, Dubna, 2006).
45. S. P. Strelkov, *Introduction to the Theory of Oscillations* (Nauka, Moscow, 1964) [in Russian].
46. L. G. Christophorou and J. K. Olthoff, "Electron interaction with plasma processing gases: An update for CF_4, CHF_3, C_2F_6 and C_3F_8," J. Phys. Chem. Ref. Data **28** (4), 967 (1999).
47. M. M. Nudnova and A. Yu. Starikovskii, presented at *IV Konferentsiya NOTs CRDF* (IV Conference of CRDF REC, MEPhI, Moscow, 2006) ISBN 5-7262-0637.
48. I. P. Kuzhekin, V. P. Larionov, and E. N. Prokhorov, *Lightning and Lightning Protection* (Znak, Moscow, 2003) [in Russian].
49. G. N. Aleksandrov, *Lightning and Lightning Protection* (Nauka, Moscow, 2008) [in Russian].
50. Yu. P. Raizer, *Gas Discharge Physics*, 3rd ed. (Izdatel'skii Dom Intellekt, Dolgoprudnyi, 2009) [In Russian].
51. *Physics of Microwaves* (Inst. Prikl. Fiz. RAN, Nizhni Novgorod, 1999), Vols. 1, 2 [In Russian].
52. Leonid I. Men'shikov, "Superradiance and related phenomena," Phys.-Usp. **42** (2), 107 (1999).
53. V. G. Shpak, M. I. Yalandin, S. A. Shunailov, N. S. Ginzburg, I. V. Zotova, A. S. Sergeev, A. D. R. Phelps, A. W. Cross, and S. M. Wiggins, "A new source of ultrashort microwave pulses based on the effect of superradiation of subnanosecond electron bunches," Dokl. Phys. **44** (3), 143 (1999).

Translated by M. Samokhina